Title
Assessment of upper tropospheric HOx sources over the tropical Pacific based on NASA GTE/PEM data: Net effect on HOx and other photochemical parameters

Journal
Journal of Geophysical Research Atmospheres, 104(D13)

ISSN
0148-0227

Authors
Crawford, J
Davis, D
Olson, J
et al.

Publication Date
1999-07-20

DOI
10.1029/1999JD900106

JOURNAL OF GEOPHYSICAL RESEARCH, VOL. 104, NO. D13, PAGES 16,255-16,273, JULY 20, 1999

Assessment of upper tropospheric HO_x sources over the tropical Pacific based on NASA GTE/PEM data: Net effect on HO_x and other photochemical parameters

J. Crawford,[1] D. Davis,[2] J. Olson,[1] G. Chen,[2] S. Liu[2], G. Gregory,[1] J. Barrick,[1] G. Sachse,[1] S. Sandholm,[2] B. Heikes,[3] H. Singh,[4] and D. Blake[5]

Abstract. Data for the tropical upper troposphere (8-12 km, 20°N-20°S) collected during NASA's Pacific Exploratory Missions have been used to carry out a detailed examination of the photochemical processes controlling HO_x ($OH+HO_2$). Of particular significance is the availability of measurements of nonmethane hydrocarbons, oxygenated hydrocarbons (i.e., acetone, methanol, and ethanol) and peroxides (i.e., H_2O_2 and CH_3OOH). These observations have provided constraints on model calculations permitting an assessment of the potential impact of these species on the levels of HO_x, CH_3O_2, CH_2O, as well as ozone budget parameters. Sensitivity calculations using a time-dependent photochemical box model show that when constrained by measured values of the above oxygenated species, model estimated HO_x levels are elevated relative to unconstrained calculations. The impact of constraining these species was found to increase with altitude, reflecting the systematic roll-off in water vapor mixing ratios with altitude. At 11-12 km, overall increases in HO_x approached a factor of 2 with somewhat larger increases being found for gross and net photochemical production of ozone. While significant, the impact on HO_x due to peroxides appears to be less than previously estimated. In particular, observations of elevated H_2O_2 levels may be more influenced by local photochemistry than by convective transport. Issues related to the uncertainty in high-altitude water vapor levels and the possibility of other contributing sources of HO_x are discussed. Finally, it is noted that the uncertainties in gas kinetic rate coefficients at the low temperatures of the upper troposphere and as well as OH sensor calibrations should be areas of continued investigation.

1. Introduction

Knowledge of upper tropospheric photochemistry is critical to understanding the global budget of tropospheric ozone and is particularly important in defining the role of ozone in climate change [e.g., *Fishman et al.*, 1979; *Wang et al.*, 1986; *Lacis et al.*, 1990; *Roelofs et al.*, 1997]. There is also great interest in the potential impact of aircraft emissions on upper tropospheric ozone [*Brasseur et al.*, 1996; *Stevenson et al.*, 1997]. Our current understanding of upper tropospheric photochemistry, however, continues to be limited for several reasons. Most notable is the lack of a comprehensive upper tropospheric database. Additionally, the role of fast vertical transport in altering the composition of the upper troposphere, while appreciated, is still difficult to quantify [e.g., *Chatfield and Crutzen*, 1984; *Dickerson et al.*, 1987; *Pickering et al.*, 1992; *Davis et al.*, 1996; *Cohan et al.*, 1999; *S. Liu et al.*, unpublished manuscript, 1999]. Still a final factor relates to the inherent uncertainties associated with the gas kinetic rate coefficients used in modeling exercises. For the low temperatures involved at upper tropospheric altitudes, many of these coefficients have significantly higher uncertainties. Taken overall, these concerns clearly suggest that the photochemical picture of the upper troposphere is one that is likely to continue to evolve.

In the last few years, many attempts to verify the key features of upper tropospheric fast photochemistry have involved the use of photochemical models constrained by airborne observations. These exercises have been largely limited to model versus observational comparisons for the species NO_2, H_2O_2, and CH_3OOH [e.g., *Crawford et al.*, 1996; *Davis et al.*, 1993, 1996; *Jacob et al.*, 1996; *Schultz et al.*, 1999; *Bradshaw et al.*, 1999]. These comparisons provided important diagnostics for indirectly assessing model estimates for the fast photochemistry of HO_x ($OH+HO_2$). More recently, direct observations of HO_2 and OH in the upper troposphere and lower stratosphere have become available (e.g., Stratospheric Tracers of Atmospheric Transport (STRAT), [*Wennberg et al.*, 1998] and Subsonic Aircraft: Contrail and Cloud Effects Special Study (SUCCESS), [*Brune et al.*, 1998]). These observations have offered an opportunity for more direct tests of HO_x photochemical theory in the upper troposphere.

With the availability of these new HO_x measurements has come the realization that the photochemistry of the upper troposphere may be more complex than previously thought. For example, model calculations of upper tropospheric HO_2 and OH levels during both the STRAT and SUCCESS campaigns have revealed that model estimated values often fall well below those

[1]NASA Langely Research Center, Hampton, Virginia.
[2]School of Earth and Atmospheric Sciences, Georgia Institute of Technology, Atlanta.
[3]Center for Atmospheric Chemistry Studies, University of Rhode Island, Narragansett.
[4]NASA Ames Research Center, Moffett Field, California.
[5]Department of Chemistry, University of California, Irvine.

Paper number 1999JD900106.
0148-0227/99/1999JD900106$09.00

measured [*Wennberg et al.*, 1998; *Jaeglé et al.*, 1997, 1998; *McKeen et al.*, 1997; *Brune et al.*,1998]. This disagreement has led to the suggestion that there may be gaps in our understanding of the chemistry in this region of the atmosphere. Such problems could exist with current mechanisms being used to model atmospheric chemistry. Alternatively, the databases being used to carry out the modeling may be inadequate either from the point of view of their being statistically non-representative of the environment being examined or in terms of their not providing the necessary constraints on model calculations. The above cited HO_x investigations focused on evaluating potential sources of HO_x previously unaccounted for in photochemical models. Sources identified in these studies that might explain the discrepancies were acetone and peroxides.

The importance of acetone as a source of HO_x in the upper troposphere was first identified by *Singh et al.* [1995] based on measurements taken during NASA's Pacific Exploratory Mission (PEM)-West B. The photolysis of acetone produces the radical species CH_3CO_3 and CH_3O_2 which, upon further reaction, can yield up to 3.2 HO_x radicals, given a high NO_x-to-HO_x environment. Additional oxygenated hydrocarbons measured by *Singh et al.* [1995] during PEM-West B were methanol and ethanol. These compounds are lost primarily through reaction with OH, and similar to many other nonmethane hydrocarbons, they can potentially serve as a net source of HO_x via further degradation of the primary radical species. Sources of oxygenated hydrocarbons are not well quantified, but include primary anthropogenic and biogenic emissions as well as secondary chemical sources from hydrocarbon oxidation [*Singh et al.*, 1994, and references therein]. Recent studies have provided evidence of particularly strong biogenic sources [*Goldan, et al.*, 1995; *Kirstine et al.*, 1998].

Peroxide compounds (e.g., H_2O_2 and CH_3OOH) have also been identified as a potential source of HO_x in the upper troposphere. The idea that peroxides might represent a source of HO_x was first proposed by *Chatfield and Crutzen* [1984], but more recently has been further explored by *Prather and Jacob* [1997] and *Jaeglé et al.* [1997,1998] in light of the new upper tropospheric HO_x measurements. Peroxides represent a rather unique source of HO_x in that there are no direct emissions of these species. Being products of photochemistry, they have not traditionally been viewed as HO_x sources. By invoking fast convective transport, however, peroxide-rich boundary layer (BL) air can be moved to the upper free troposphere. In this case, peroxide species could be enhanced above what might be expected if their only source were local photochemistry. One can argue that this condition should be more likely for CH_3OOH since it is relatively insoluble [*O'Sullivan et al.*, 1996] as compared to H_2O_2.

Although the STRAT and SUCCESS programs have opened up new opportunities for testing HO_x photochemical theory, both programs have lacked the supporting measurements of acetone and peroxides necessary for more conclusive results. The STRAT and SUCCESS studies have relied heavily on observations from NASA's recent Pacific Exploratory Missions (PEM) to infer possible levels of acetone and peroxides. This investigation examines the photochemical consequences of constraining model calculations with measurements of acetone, methanol/ethanol, and peroxides, as well as other critical photochemical parameters recorded during NASA's PEM missions. Of specific interest will be the upper tropospheric tropical data.

2. Observational Database

The data used in this analysis were recorded in the upper troposphere (8-12 km) over the tropical North and South Pacific Oceans. This region was visited on three separate occasions during NASA's Pacific Exploratory Missions: PEM-West A (PWA), September-October 1991; PEM-West B (PWB), February-March 1994; and PEM-Tropics A (PTA), August-October 1996. Figure 1 shows the geographic coverage of these campaigns. The PWA and PWB missions overlapped in the North Pacific, whereas PTA primarily sampled in the South Pacific. With some minor exceptions, the suite of measurements available to constrain the model calculations was the same for each flight campaign [*Hoell et al.*, 1996, 1997, 1999]. Equally important is the fact that the investigators and measurement techniques were nearly the same for all three campaigns. In addition to the standard photochemical modeling parameters (e.g., O_3, CO, NO, dew/frost point, NMHCs), observations were also reported for the centrally important labile oxygenated species H_2O_2, CH_3OOH, acetone, methanol, and ethanol, the latter three species being measured only in PWB.

Modeling results for PWA, PWB, and PTA have been based on merged data sets produced by S. Sandholm at the Georgia Institute of Technology. These merges are available by anonymous FTP from ftp://lif.gtri.gatech.edu/pub. Since each of these merges has a different time base (3 min, PWA; 30 s, PWB; and 60 s, PTA), adjustments have been made to provide a uniform statistical database spanning all three campaigns. The approach taken involved weighting the data such that the 30 s PWB data were counted once, the 60 s PTA data were counted twice, and the 3 min PWA data were counted six times. This

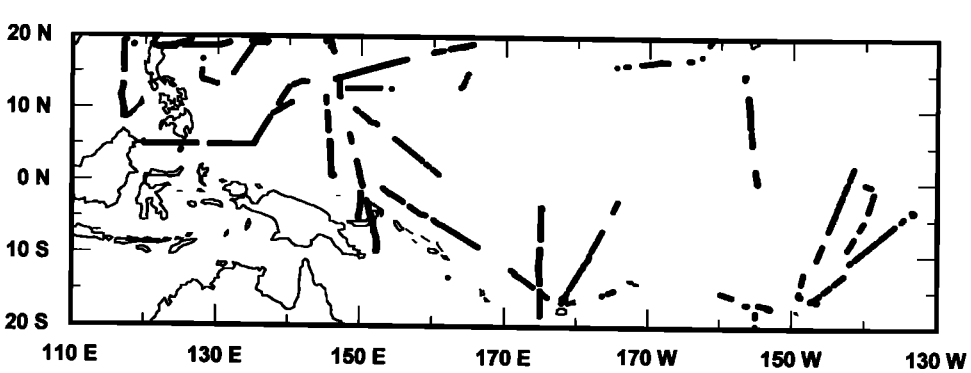

Figure 1. Geographic distribution of tropical upper tropospheric (8-12 km) data for PWA, PWB, and PTA.

Table 1. Distribution of Flight Data

Altitude	Flight Duration
8-9 km	9 hours, 20 min
9-10 km	8 hours, 56 min
10-11 km	6 hours, 18 min
11-12 km	2 hours, 16 min

procedure ensured that median statistics for the database were representative of the actual sampling times involved. Table 1 gives the size of the PEM database between 8-12 km. For this analysis, the data have been grouped into four altitude ranges of 1 km thickness.

The basic chemical input parameters O_3, CO, NO, and H_2O were available for all model calculations. Distributions for these constituents are shown in Figure 2. Concurrent NMHC observations were available for only 50% of the data. Gaps in these observations were treated as previously described by *Davis et al.* [1996] and *Crawford et al.* [1996, 1997b]. Interpolated values were used for 43% of the data with the remaining 7% being assigned regional median values for specific altitude bands.

2.1. Water Vapor

Water vapor measurements were available from three different instruments. For PWA, high-altitude water vapor data were those measured by Lyman-α fluorescence. For PWB, the data from a cryogenically cooled, chilled-mirror hygrometer [*Busen and Buck*, 1995] was used. During PTA, cryogenic hygrometer measurements were again available, but diode laser measurements of water vapor [*Vay et al.*, 1998] were also recorded. The diode laser measurements which were available for ~60% of the high-altitude data provided an opportunity to examine the potential range of uncertainty in water vapor measurements. As noted by *Schultz et al.* [1999], agreement between the two sensors was quite good for mixing ratios above 100 ppmv (e.g., ±30%). Below 100 ppmv, however, the diode laser was consistently higher than the cryogenic hygrometer by an average difference of 28 ppmv, with over 70% of the data differing by 20-40 ppmv. Given the low water vapor at 11-12 km (see Figure 2), the diode laser measured water vapor exceeded that reported by the cryogenic hygrometer by factors ranging from 2.5 to 4.7.

Since both of these systems have previously demonstrated the capability for measuring water vapor at tens of ppmv, this work does not attempt to resolve the discrepancy. Instead, data from

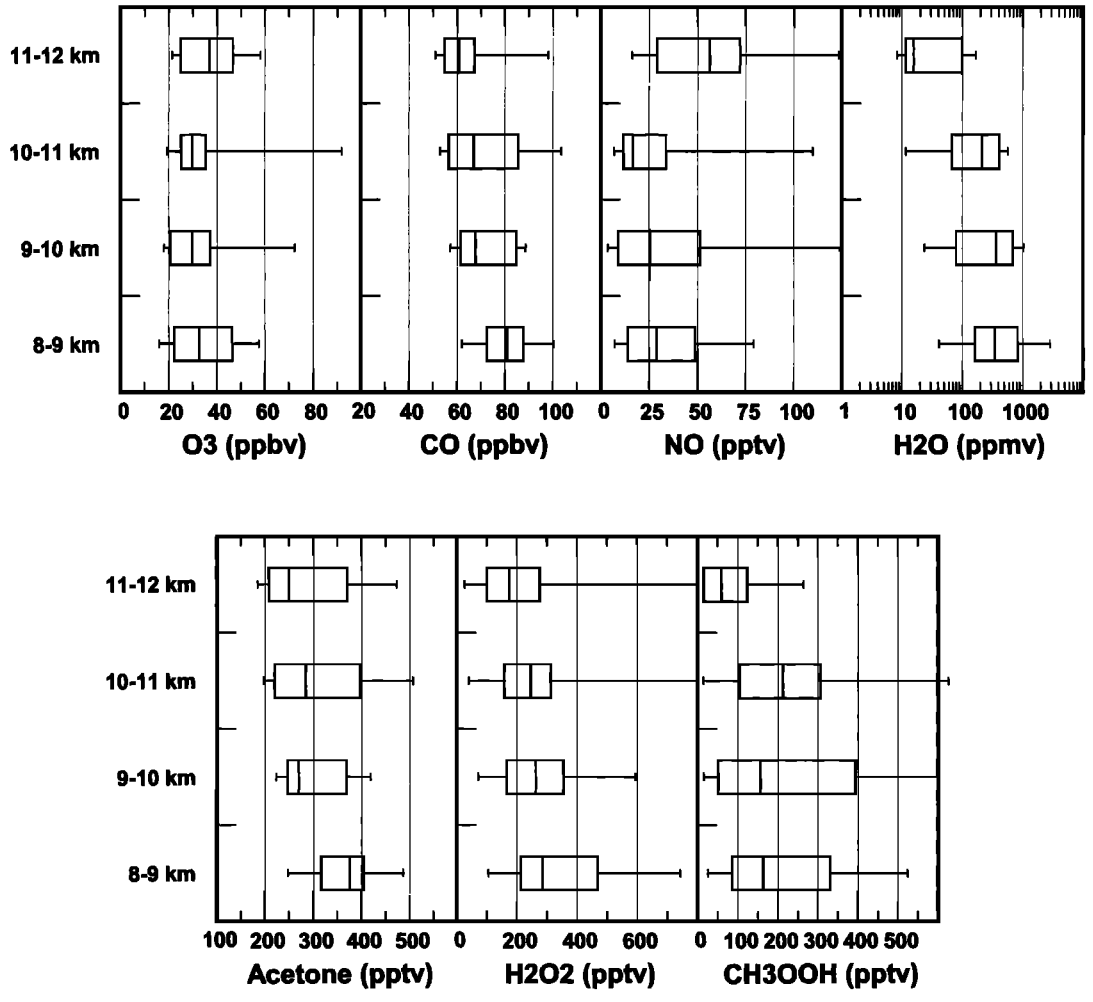

Figure 2. Distributions for key atmospheric constituents. The center line denotes the median value, boxes encompass the inner quartiles, and whiskers encompass to 5th and 95th percentiles.

the cryogenic hygrometer have been used since this system was operated during both PTA and PWB and also provided a larger database. However, calculations based on the diode laser water vapor are discussed later in the text. The water vapor distribution shown in Figure 2 is that defined by the cryogenic hygrometer for PWB and PTA and that recorded by the Lyman-α fluorescence instrument during PWA.

2.2. Oxygenated Hydrocarbons

Oxygenated hydrocarbon measurements were available only for PWB [*Singh et al.*, 1995]. These measurements suggested, however, that acetone, methanol, and ethanol are ubiquitous in the tropical upper troposphere. As a result, they have been used to infer acetone concentrations in a number of other studies [*McKeen et al.*, 1997; *Jaeglé et al.*, 1997, 1998]. For purposes of this study, acetone for PWA and PTA has also been inferred to allow maximum usage of the PEM database. Acetone values were inferred according to the analysis of *McKeen et al.* [1997] which revealed a strong correlation between acetone and CO in the upper tropospheric PWB data. In this study, inferred acetone values were used for 83% of the data analyzed. The distribution of acetone used in these calculations is shown in Figure 2.

Methanol and ethanol were also inferred according to the PWB observations. These observations showed methanol exceeding acetone in all cases with an average methanol-to-acetone ratio of 1.5. Thus, in those cases where acetone was inferred, the mixing ratio for methanol was taken to be a factor of 1.5 times larger. While ethanol was also shown to have measurable concentrations in the upper troposphere during PWB, concentrations were considerably more variable, and its short lifetime in the upper troposphere (~5 days) renders it far less predictable than either acetone or methanol. For this reason, a constant mixing ratio of 30 pptv was used when a measurement of ethanol was not available. This value is on the conservative side given that more than 85% of the high-altitude ethanol measurements exceeded this level.

2.3. Peroxides

The peroxide species H_2O_2 and CH_3OOH were measured in all three campaigns [*Heikes et al.*, 1996; *O'Sullivan et al.*, 1999]. Unlike the oxygenated hydrocarbons, peroxide species could not be easily inferred for gaps in the data; thus, the data used in this analysis were limited to those time periods for which measurements were available. The distribution of peroxides is given in Figure 2. This includes those periods when peroxides were at or below the limit of detection (LOD). LOD values for H_2O_2 and CH_3OOH were 15 and 25 pptv, respectively. While the uncertainty in these measurements varies with concentration, the typical uncertainty for the data used here is ±30%. Note, while H_2O_2 was measured at LOD values for less than 2% of the data, LOD values for CH_3OOH comprise 12% of the data. Furthermore, 42% of the CH_3OOH data at 11-12 km were LOD.

3. Model Description

Data analysis for this study involved the use of a time dependent photochemical box model similar to that used for previous PEM related work [*Davis et al.*, 1993, 1996; *Crawford et al.*, 1996, 1997a, b]. The model mechanism has been updated to reflect the most current reactions and rate coefficient recommendations [*DeMore et al.*, 1997; *Atkinson et al.*, 1992] and includes basic HO_x-NO_x-CH_4 gas phase chemistry, nonmethane hydrocarbon (NMHC) chemistry, photolysis reactions, and heterogeneous loss for soluble species. A detailed listing of reactions and rate coefficients are contained in the appendix. The NMHC chemistry is based on the condensed mechanism of *Lurmann et al.* [1986] with modifications that include appropriately updated rate coefficients, additional reactions for remote low-NO_x environments (e.g., formation of organic peroxides), and explicit chemistry for some species previously "lumped" into families (e.g., acetone, propane, and benzene). Photolysis rate coefficients are based on a DISORT 4-stream implementation of the NCAR Tropospheric Ultraviolet-Visible (TUV) radiative transfer code (S. Madronich, private communication). A more detailed description of the photolysis rate coefficient calculations is given by *Crawford et al.* [1999].

Model calculations are constrained by observations of O_3, CO, NO, NMHCs, temperature, dew point, and pressure. When measurements are available, model calculations can also be constrained by the following species: H_2O_2, CH_3OOH, HNO_3, PAN, acetone, CH_3OH, C_2H_5OH, HCOOH, and CH_3COOH. With the exception of NO, constraining parameters are assumed to be constant over the diurnal cycle. NO is allowed to vary diurnally; however, total short-lived nitrogen ($NO+NO_2+NO_3+2N_2O_5+HONO+HO_2NO_2$) is held constant. The amount of short-lived nitrogen is determined such that the NO concentration matches the measurement at the appropriate time of day. Photochemistry dictates the partitioning of short-lived nitrogen among the constituent species.

Model-calculated species are assumed to be at steady state, meaning that concentrations were integrated in time until their diurnal cycles no longer varied from day to day. Results presented here are based on diurnal average values for calculated species and photochemical rates.

4. Approach

Assessing the impact of individual HO_x sources in the upper troposphere is complicated by the fact that the system is highly nonlinear. One approach taken in earlier studies has involved looking at primary source strengths for individual pathways [*Wennberg et al.*, 1998; *Jaeglé et al.*, 1997]. While this does provide an indication of the relative importance of various HO_x sources, it does not fully address the most pivotal question concerning the final impact on HO_x concentrations. In the upper troposphere, HO_x tends to be regulated not by primary sources, but by secondary formation through the oxidation of CH_4 and other NMHCs [*Liu et al.*, 1980]. Additionally, some of the most important sink processes for HO_x are quadratic losses (HO_2+HO_2, HO_2+OH); thus, absolute HO_x concentrations are not very sensitive to changes in primary production rates. This can be most clearly demonstrated with an example based on actual PEM flight data. A specific data sample from PTA flight 17 was chosen with the following conditions: 8.7 km, 38 ppbv O_3, 80 ppbv CO, 100 pptv NO, 93 ppmv H_2O, and 363 pptv acetone. Based on these input conditions, three calculations were conducted. The first considered only the impact of primary production of HO_x from water vapor. The second included only primary production from acetone. The predicted HO_x for these two calculations was identical (i.e., 2.45×10^7 molecules/cm^3). In a third calculation which included both primary sources, the predicted HO_x increased to 2.92×10^7 molecules/cm^3. Thus, when combined, these two HO_x sources resulted in only 20% more HO_x than each could produce by itself in isolation. This result can only be understood when the importance of secondary HO_x formation is examined.

Secondary formation of HO_x is initiated by the oxidation of CH_4 (or some other hydrocarbon species) by OH to form organic peroxy radicals, e.g.:

(R1) $CH_4 + OH \rightarrow CH_3 + H_2O$
(R2) $CH_3 + O_2 \rightarrow CH_3O_2$

In the presence of NO, these organic peroxy radicals can react to form HO_2 and formaldehyde (CH_2O), e.g.:

(R3) $CH_3O_2 + NO \rightarrow CH_3O + NO_2$
(R4) $CH_3O + O_2 \rightarrow CH_2O + HO_2$

Through photolysis, formaldehyde can yield additional HO_2:

(R5) $CH_2O + h\nu \rightarrow CHO + H$
(R6) $CHO + O_2 \rightarrow HO_2 + CO$
(R7) $H + O_2 \rightarrow HO_2$

For the first sample calculation discussed above, the diurnal average primary HO_x source from water vapor (i.e., $O(^1D)+H_2O$) was approximately 8×10^3 molecules cm^{-3} s^{-1}. The secondary formation rate resulting from the combination of (R3) and (R5) totaled 4.5×10^4 molecules cm^{-3} s^{-1}. Thus, primary production constituted only about 15% of the total HO_x formation rate. In the case of the second calculation, CH_3O_2 and CH_2O resulting from acetone photolysis versus methane oxidation had to be differentiated, but the same result (i.e., 8×10^3 versus 4.5×10^4 molecules cm^{-3} s^{-1}) was determined. In the third calculation, the combination of primary sources doubles primary formation, but the increase in secondary formation depends on the increase in OH which is small given the quadratic loss of HO_x. Thus, the total formation rate of HO_x in the third calculation is only about 35% greater than that for the first two calculations despite a doubling in primary production.

For purposes of this study, an approach has been taken that does not attempt to evaluate the relative importance of individual primary sources. Rather, a series of sensitivity calculations has been conducted to evaluate how predictions of HO_x and related photochemical parameters change for successive degrees of model constraint. This sensitivity analysis examines the incremental change in model calculations based on PEM data by constraining the model according to the following progression: (1) water vapor, (2) NMHCs, (3) acetone, (4) methanol/ethanol, (5) CH_3OOH, and (6) H_2O_2. As demonstrated above, the order in which these constraints are invoked cannot be construed as any indication of their relative importance in terms of primary production of HO_x; however, there are other procedural reasons for choosing this order.

Water vapor is considered first. Through $O(^1D)+H_2O$, it represents the most basic HO_x precursor that is universally considered in all models; thus, any changes to our current understanding of upper tropospheric HO_x chemistry should be referenced to how these modifications alter this basic chemistry. NMHCs are considered next since they also represent an input to models that has been well recognized. They sometimes are neglected in the upper troposphere due to low concentrations, but they still represent a basic component of most photochemical models.

Acetone represents a more recently recognized addition to the basic photochemistry of the upper troposphere. Since the work of *Singh et al.* [1995], the impact of acetone has been considered in several photochemical analyses of NASA GTE data [*Davis et al.*, 1996; *Jacob et al.*, 1996; *Crawford et al.*, 1997a, b; *Schultz*

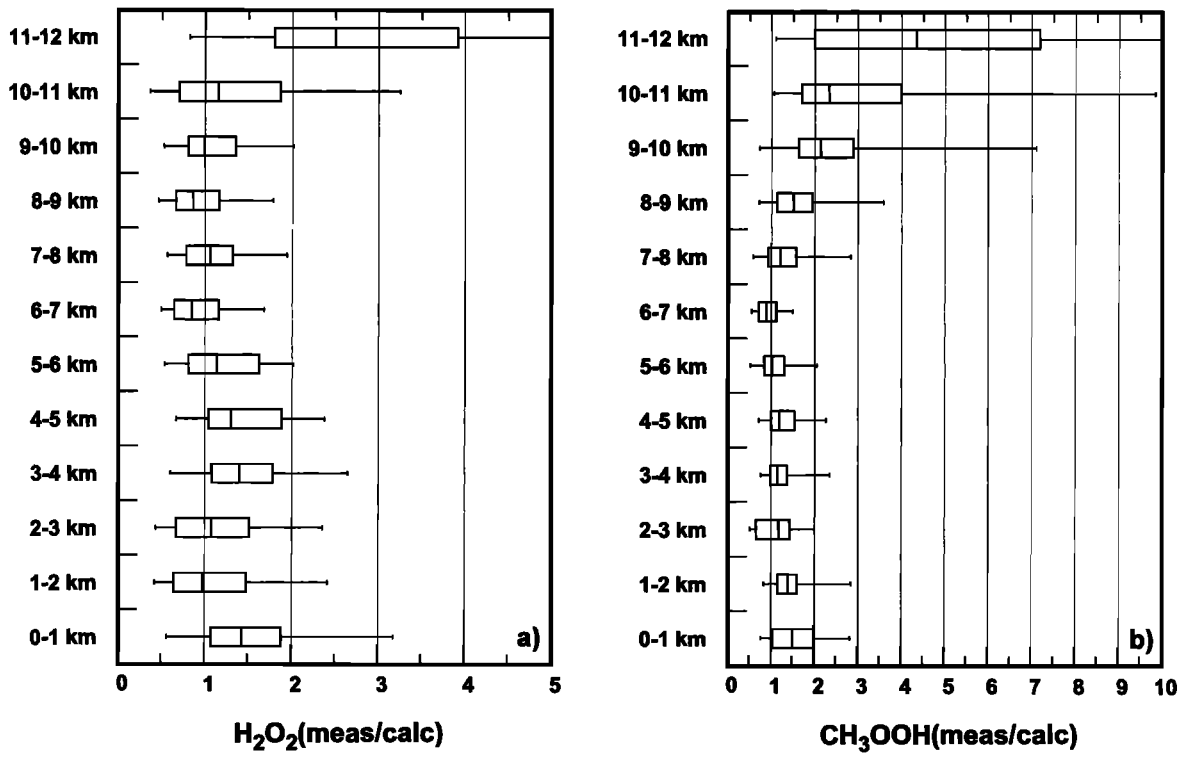

Figure 3. Box-whisker plot of (a) H_2O_2(meas/calc) and (b) CH_3OOH(meas/calc). See Figure 2 for box-whisker definition.

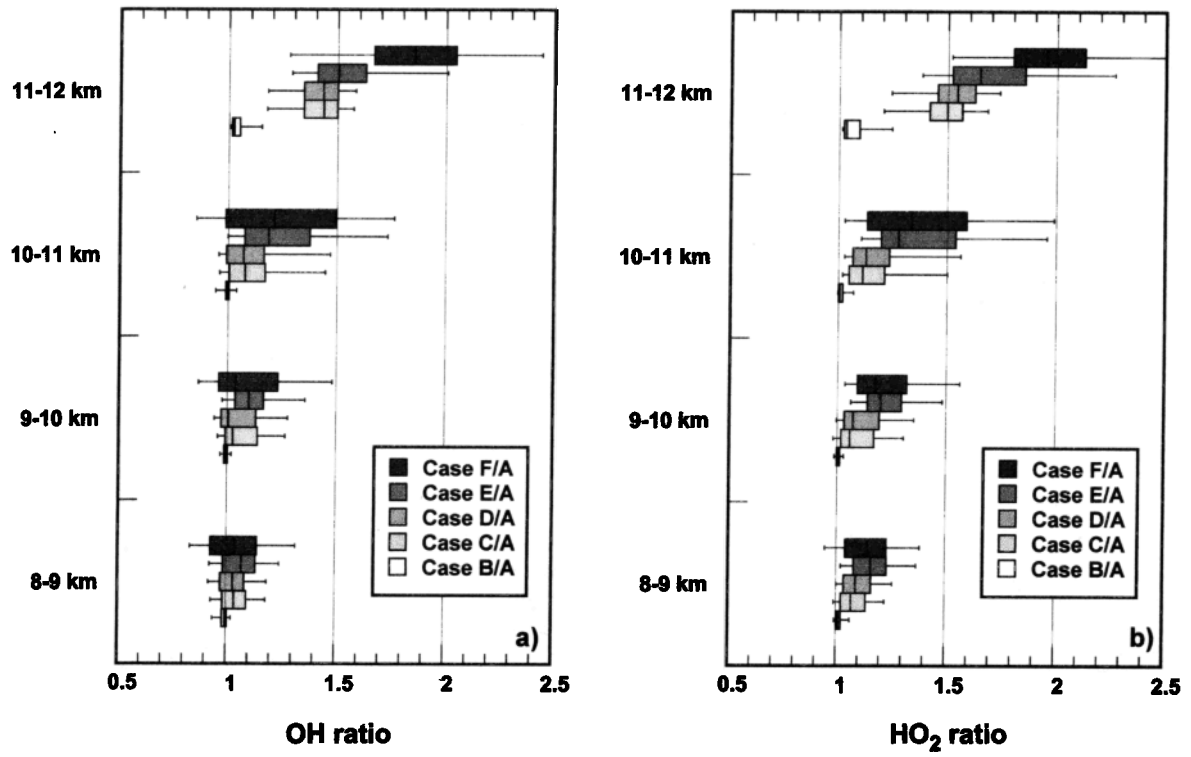

Figure 4. Box-whisker plots of model sensitivity calculations normalized to the "standard" case (case A) for (a) OH and (b) HO_2. See Figure 2 for box-whisker definition.

et al., 1999]. Given its ubiquitous nature and correlation with CO, reasonable mixing ratios can be incorporated into model calculations with little effort. Similarly, methanol and ethanol are added to more completely evaluate the impact from oxygenated hydrocarbons.

Peroxides are considered last due to their transient nature. Since they are short-lived, it is expected that their enhancements in the upper troposphere are limited in space and time by the stochastic nature of convective events. Unlike the other constraining species, peroxides can be estimated from a model based on photochemical equilibrium considerations in the absence of measurements. Constraining the model with peroxides must therefore be viewed as a deviation from photochemical equilibrium as defined by observations. Such an adjustment could take the form of either an increase or decrease in peroxide mixing ratios. To demonstrate this, Figure 3 shows box-whisker plots of measured-to-calculated peroxide ratios for all tropical PEM data. In this case, the calculated values are based on model runs that have been constrained by all measured variables other than the peroxides. Since this evaluation is in the form of a ratio, only those measurement periods where peroxide levels were above the LOD are shown. These results show that H_2O_2 is reasonably well predicted, i.e., the median ratio is near unity. Furthermore, there appears to be no significant trend in the ratio with increasing altitude, the exception being the data at 11-12 km. By contrast, values for the CH_3OOH ratio exhibit a strong altitude trend, especially above 8 km. Potential explanations for these trends in H_2O_2 and CH_3OOH will be explored later in the discussion of results.

5. Results

The modeling results that follow are presented as a series of cases beginning with the "standard" case of basic photochemistry constrained only by measured values of O_3, CO, NO, and H_2O (case A). Subsequent modeling runs, referred to as cases B-F, represent the sequential addition of NMHCs (case B), acetone (case C), methanol and ethanol (case D), CH_3OOH (case E), and H_2O_2 (Case F). This allows for an examination of the incremental changes in predicted HO_x levels and related parameters as the number of constraint species is progressively increased. For cases A-D, CH_3OOH and H_2O_2 have been calculated to be in photochemical equilibrium. For all LOD peroxide values, these species continue to be calculated based on photochemical equilibrium conditions for cases E and F. The median calculated CH_3OOH and H_2O_2 values for LOD measurements were 30 and 95 pptv, respectively.

Figures 4-6 show how the successive addition of constraints influence calculated levels of HO_x and related photochemical parameters. These changes are represented by the ratio for each case relative to case A. Table 2 gives the overall median and mean change for each species or parameter (i.e., case F/case A). To accompany the discussion of results, Table 3 outlines the most relevant reactions associated with each HO_x source.

5.1. HO_x (OH and HO_2)

Figures 4a and 4b illustrate that increases in HO_x due to changes in model constraints tend to be greatest at higher altitudes. This trend is consistent with the decrease in water vapor with increasing altitude, and thus, a reduction in the contribution from the $O(^1D)+H_2O$ source. Although OH and HO_2 are in rapid photochemical equilibrium, Figures 4a and 4b reveal that their respective responses to changing model constraints are not identical. Table 2 also shows that below 10 km median increases in HO_2 are nearly 3 times greater than those for OH. Only at 11-12 km do changes in OH approach those calculated for HO_2.

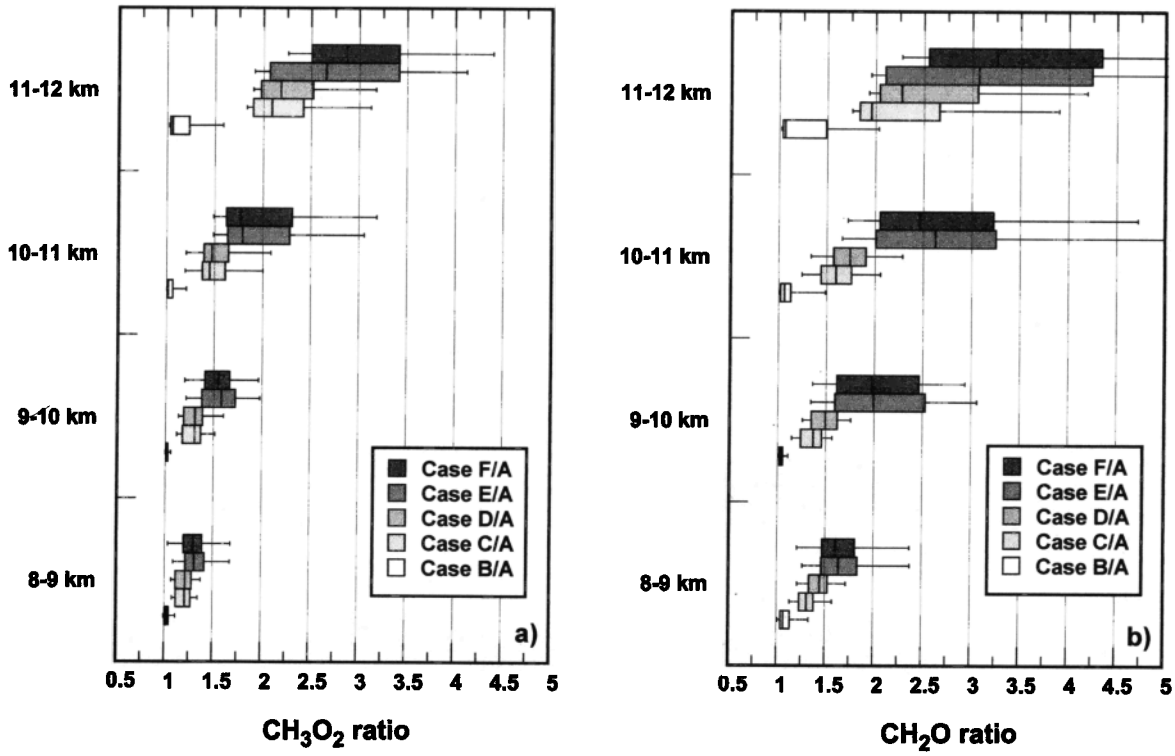

Figure 5. Box-whisker plots of model sensitivity calculations normalized to the "standard" case (case A) for (a) CH_3O_2 and (b) CH_2O. See Figure 2 for box-whisker definition.

The muted response of OH appears to be related to a combination of factors. Most obvious is the additional burden on OH presented by the constraints associated with cases B-F. This is particularly true for NMHCs, methanol, and ethanol which are principally lost through reaction with OH. Acetone and CH_3OOH react with OH as well, but they also have important losses through photolysis. Another factor relates to the potential for HO_x cycling. Unlike $O(^1D)+H_2O$ and $H_2O_2+h\nu$ which introduce HO_x in the form of OH, the other HO_x sources initially form HO_2. Thus, for those environments where ambient HO_x and NO_x levels are comparable, it becomes more likely that HO_2 will be lost to either self-reaction or reaction with other organic peroxy radicals before being cycled into OH via reaction with NO.

Below 11 km, the largest changes in HO_x levels are associated with acetone and CH_3OOH. NMHCs, methanol, and ethanol appear to exert a minimal influence both on HO_2 and OH. H_2O_2 also shows little impact below 11 km; however, the range of values is broadened. Above 11 km, H_2O_2 has a greater impact than CH_3OOH, and acetone continues to be a strong influence. Since H_2O_2 introduces HO_x in the form of OH, it also helps explain why increases in OH approach those for HO_2 at this altitude.

5.2. CH_3O_2 and CH_2O

CH_3O_2 and CH_2O represent two important intermediate products in the formation of HO_x from the oxidation of NMHCs, acetone, methanol, ethanol, and CH_3OOH. Figures 5a and 5b show that shifts in the ratio for these species are significantly larger than those for OH and HO_2. The larger response for these species is expected since the follow-on chemistry for each does not automatically lead to HO_2 formation. This is particularly true for the radical species CH_3O_2 when the environment is NO_x poor. Formaldehyde also has alternate degradation pathways that do not produce HO_2 (see Table 3).

The largest shifts in the ratio for CH_3O_2 and CH_2O are associated with acetone and CH_3OOH; however, for CH_2O, methanol and ethanol also make a significant contribution. H_2O_2 has relatively little impact on CH_3O_2 and CH_2O, even at 11-12 km. As was observed for OH and HO_2, the overall changes for both CH_3O_2 and CH_2O increase with altitude. Of the two, CH_2O is clearly the most sensitive species, making it an ideal candidate in testing for the presence of additional HO_x sources.

5.3. Ozone Budget

Impacts on the ozone budget are depicted in Figure 6. Shifts in the ozone budget are coupled directly to changes in HO_x levels. Ozone formation, $F(O_3)$, which is driven by the reaction of NO with peroxy radicals is strongly dependent upon HO_2 and, to a lesser degree, CH_3O_2 and other organic peroxy radicals. This is reflected in Table 2 which shows that median increases in $F(O_3)$ exceed enhancements in HO_2 but are less than those for CH_3O_2. On the other hand, $D(O_3)$ depends only partially on HO_2 and OH; thus, increases in its median value are smaller than those for HO_2. In the upper free troposphere, $F(O_3)$ typically exceeds $D(O_3)$; therefore, the net ozone tendency, $P(O_3)$, tends to be positive and to track $F(O_3)$. Median increases in $P(O_3)$ are similar to, but slightly larger than, those for $F(O_3)$.

6. Discussion

Similar to previous studies, these results clearly demonstrate that model-calculated values of HO_x for the upper troposphere based solely on the $H_2O+O(^1D)$ source will lead to an underestimate of HO_x levels. Furthermore, these underestimates may be even larger for related quantities such as gross and net

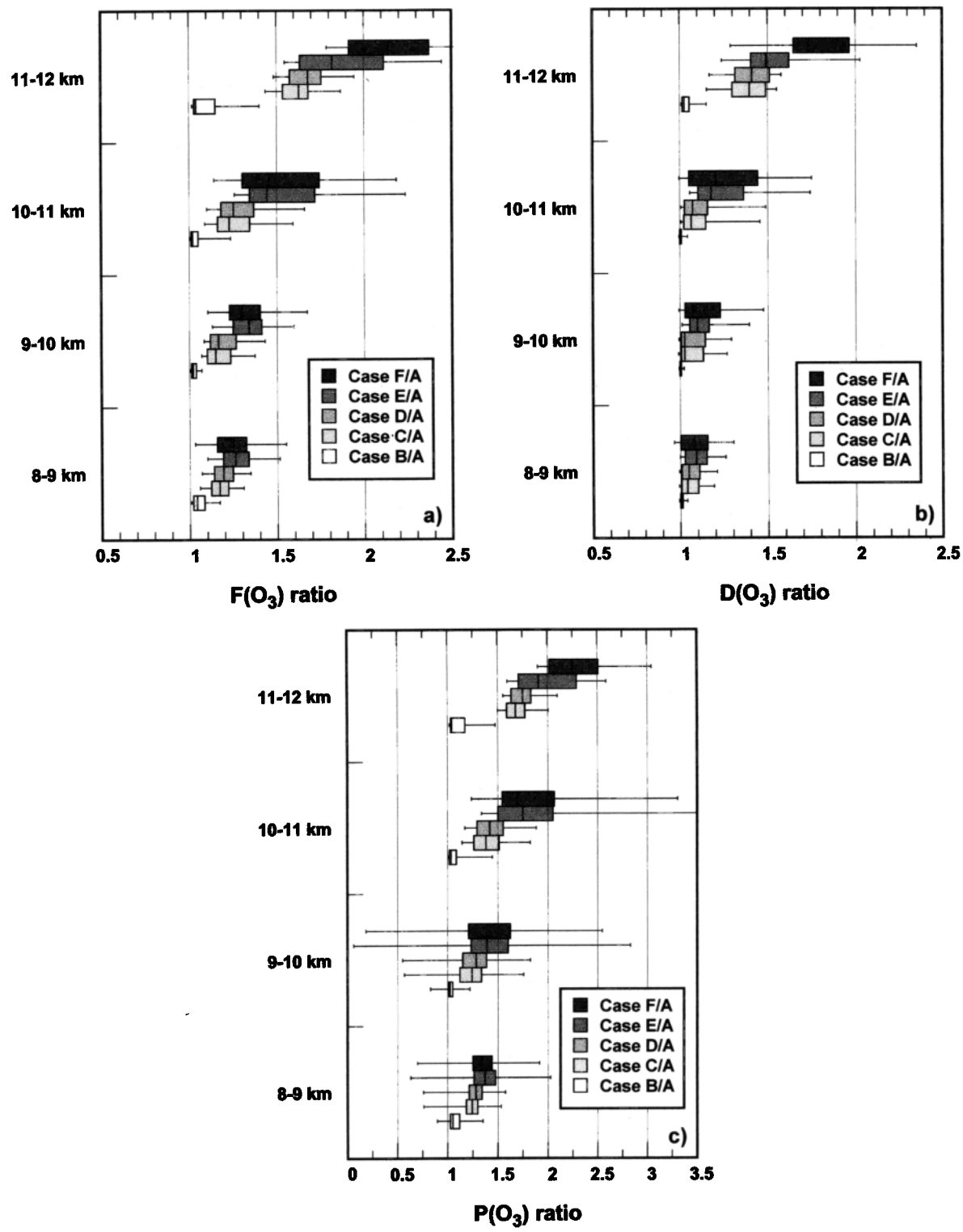

Figure 6. Box-whisker plots of model sensitivity calculations normalized to the "standard" case (case A) for (a) $F(O_3)$, (b) $D(O_3)$, and (c) $P(O_3)$. See Figure 2 for box-whisker definition.

ozone production. Even so, the increases in calculated HO_x for the PEM data, especially increases due to peroxides, appear to be significantly less than what might be expected based on recent HO_x measurements [*Wennberg et al.*, 1998; *Brune et al.*, 1998; *Jaeglé et al.*, 1997, 1998]. Thus, the current model results raise several key questions: (1) While water vapor alone can sustain most of the calculated HO_x, how well does one need to know the measured water vapor level? (2) If peroxides are influencing upper tropospheric HO_x through convection, why does H_2O_2 rather than CH_3OOH have the greater influence?, and (3) What

Table 2. Overall Changes in Tropical Upper Tropospheric Photochemical Parameters (case F/case A)

	OH	HO_2	CH_3O_2	CH_2O	$F(O_3)$	$D(O_3)$	$P(O_3)$
8-9 km							
Median	1.04	1.14	1.30	1.61	1.25	1.08	1.34
Mean	1.04	1.15	1.31	1.69	1.25	1.09	1.35
9-10 km							
Median	1.04	1.17	1.55	1.98	1.30	1.08	1.39
Mean	1.11	1.22	1.56	2.06	1 33	1.14	1.76
10-11 km							
Median	1.21	1.34	1.77	2.47	1.46	1.20	1.70
Mean	1.25	1.40	2.03	2.85	1.56	1.27	1.85
11-12 km							
Median	1.86	1.95	2.87	3.26	2.14	1.73	2.25
Mean	1.87	1.98	3.12	3.73	2.18	1.78	2.30

other HO_x sources might play a role in upper tropospheric chemistry? Below, we explore each of these questions in the context of the GTE-PEM observations and modeling results.

6.1. Water Vapor

Earlier discussion of water vapor observations from PTA revealed that measurements have a very high uncertainty below 100 ppmv (e.g., factors of 3-5). This conclusion was based on a comparison of cryogenic hygrometer and diode laser observations. The issue of water levels becomes especially important with respect to calculations at altitudes of 11-12 km where sensitivity calculations showed model constraints to have their greatest impact. Additional calculations for the PTA data at 11-12 km were conducted based on diode laser water vapor to examine the impact of this uncertainty.

An initial set of calculations was based on chemistry considering only the diode laser water observations (i.e., case A). Relative to "case A" calculations for the cryogenic hygrometer, OH and HO_2 values were about 30% larger. This represents a small change given that increases in primary production of HO_x were factors of 3 to 5. These results further highlight the earlier point that HO_x tends to be fairly insensitive to changes in primary production at these altitudes. These calculations also make the strong point that relatively small errors in the measurement of HO_x levels can lead to the conclusion that there is a need for a large change in primary production.

Calculations were also carried out based on the diode laser water measurements together with all other model constraints (i.e., case F). Relative to calculations based on the cryogenic

Table 3. Sources of HO_x and Competing Reactions

Sources of HO_x	Competing Reactions
Ozone Photolysis	
$O_3+h\nu \rightarrow O(^1D)+O_2$	
$O(^1D)+H_2O \rightarrow 2OH$	$O(^1D)+M \rightarrow O(^3P)+M$
Nonmethane Hydrocarbon Oxidation	
$RH+OH \xrightarrow{O_2} RO_2+H_2O$	
$RO_2+NO \xrightarrow{O_2} RCHO+HO_2+NO_2$	$RO_2+HO_2 \rightarrow ROOH+O_2$
$RCHO+h\nu \xrightarrow{O_2} RO_2+HO_2+CO$	$RCHO+OH \xrightarrow{O_2} RCO_3+H_2O$
Acetone Photolysis	
$CH_3C(O)CH_3+h\nu \xrightarrow{O_2} CH_3CO_3+CH_3O_2$	
$CH_3CO_3+NO \xrightarrow{O_2} CH_3O_2+NO_2+CO$	$CH_3CO_3+HO_2 \rightarrow ROOH+O_2$/Acetic Acid$+O_3$ $CH_3CO_3+NO_2 \rightarrow PAN$
$CH_3O_2+NO \xrightarrow{O_2} CH_2O+HO_2+NO_2$	$CH_3O_2+HO_2 \rightarrow CH_3OOH$
$CH_2O+h\nu \xrightarrow{O_2} 2HO_2+CO$	$CH_2O+h\nu \rightarrow CO+H_2$ $CH_2O+OH \xrightarrow{O_2} HO_2+CO+H_2O$
Methanol/Ethanol Oxidation[a]	
$CH_3OH+OH \xrightarrow{O_2} CH_2O+HO_2+H_2O$	
$C_2H_5OH+OH \xrightarrow{O_2} CH_3CHO+HO_2+H_2O$	
$CH_3CHO+h\nu \rightarrow CH_3O_2+HO_2+CO$	$CH_3CHO+OH \rightarrow CH_3CO_3+H_2O$
CH_3OOH Photolysis[b]	
$CH_3OOH+h\nu \xrightarrow{O_2} CH_2O+HO_2+OH$	
$CH_3OOH+OH \rightarrow CH_2O+OH+H_2O$	$CH_3OOH+OH \rightarrow CH_3O_2+H_2O$
H_2O_2 Photolysis	
$H_2O_2+h\nu \rightarrow 2OH$	$H_2O_2+OH \rightarrow HO_2+H_2O$

[a]see acetone for subsequent reactions of CH_3CO_3, CH_3O_2, and CH_2O
[b]see acetone for subsequent reactions of CH_3O_2 and CH_2O

hygrometer measurements, OH and HO_2 values increased by only 5% on average. Thus, HO_x levels are indicated to be relatively insensitive to the absolute water level in the upper troposphere (11-12 km), reflecting the dominance of secondary production as well as the fact that water is less important as a primary source than acetone.

6.2. Peroxides

Understanding the role that peroxides play in upper tropospheric photochemistry is complicated by the fact that these species are derived not only from local photochemistry but also from transport. Thus, observations of these species in the upper troposphere must be viewed as the net result from some combination of both sources. Box models can only assess the levels of peroxides expected from local photochemistry. Thus, any impact due to transport (e.g., deep convection) must be inferred through comparisons of measured and calculated peroxide levels. Convective transport of peroxides cannot be realistically identified by only comparing differences in the measured peroxide mixing ratios between two air masses. This is demonstrated by a close examination of the PWB data for the tropical upper troposphere. This data has been used in recent studies to infer convective transport of peroxides [*Jaeglé et al.*, 1997; *Folkins et al.*, 1998]. For example, *Jaeglé et al.* compared PWB peroxides for convected and background air using dimethyl sulfide as a convective tracer. When levels were above 3 pptv, the air mass was assumed to be one which had been strongly influenced by deep convection. *Folkins et al.* made a similar comparison of PWB peroxide levels but based their assessment on NO levels. For air masses with NO below 25 pptv, it was assumed that the air mass had been significantly influenced by recent marine convection. Both approaches led to the conclusion that convection had enhanced both H_2O_2 and CH_3OOH by factors of 2-3 and 5-6, respectively. Not recognized, however, was the difference in water vapor for the two air mass types.

Crawford et al., [1997a] discussed in some detail the tropical PWB data used by *Jaegle et al.*, and *Folkins et al.*, dividing it into what were labeled "high NO_x" and "low NO_x" regimes. *Crawford et al.* argued that both regimes resulted from recent convection, one of continental origin (high NO_x) and the other of marine origin (low NO_x). Among the important differences cited was the large difference in water vapor between these regimes. The data in Table 4 show that much of the difference in peroxide levels for these two regimes can be explained by differences in the local chemical environment rather than transport of peroxides from the marine boundary layer. The median values for the ratio of measured-to-calculated H_2O_2 for both regimes suggest that the local photochemical environment could easily sustain the observed H_2O_2 mixing ratios without invoking transport (see Table 4). The higher H_2O_2 levels in the low NO_x regime appear to be the result of both higher water vapor leading to increased HO_x levels and lower NO leading to less HO_x cycling, and hence, increased formation of H_2O_2. This interpretation of the data would seem to be in better accord with the known high solubility of H_2O_2 and would argue against H_2O_2 being effectively transported to the upper troposphere by deep convection.

By contrast, Table 4 shows that median values for the ratio of measured-to-calculated CH_3OOH are greater than unity for both regimes. This suggests that in the case of CH_3OOH there could be a role for convective transport. The low NO_x regime is shown to have the higher median ratio (i.e., 2.16 vs 1.57); however, this difference in ratios falls far short of explaining the factor of 5 difference in median levels of CH_3OOH which again appear to be largely attributable to differences in local photochemistry.

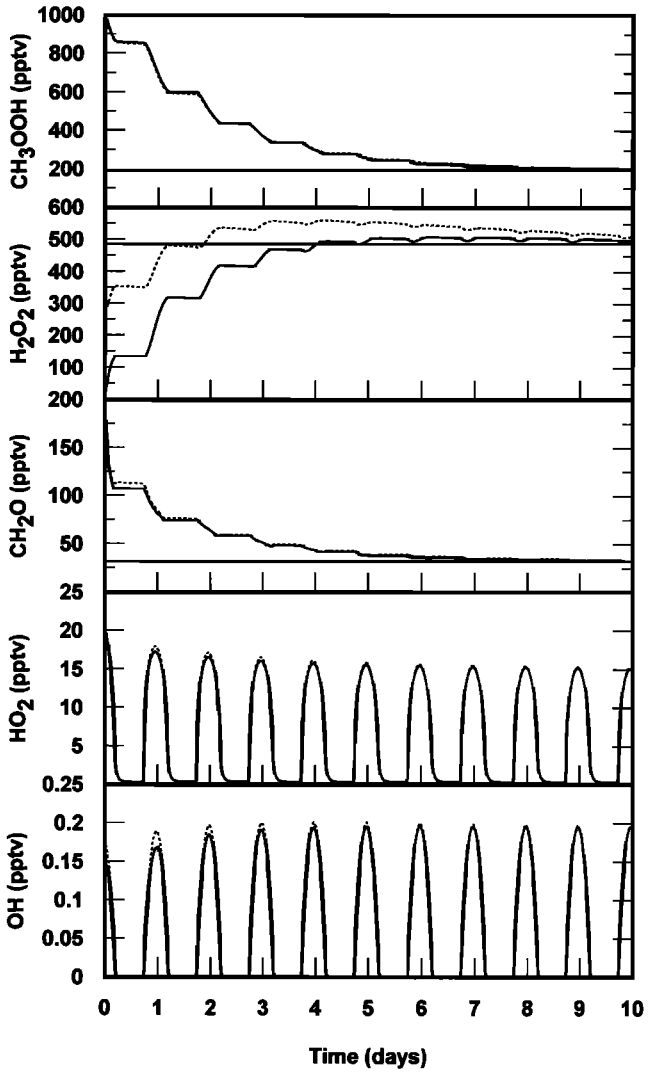

Figure 7. Time evolution of convectively perturbed peroxides and CH_2O for median conditions observed in the low NO_x regime of PEM-West B. Perturbations consist of typical marine boundary layer values for CH_3OOH (1 ppbv) and CH_2O (200 pptv). Solid lines represent the assumption of total scavenging of H_2O_2. Dotted lines assume H_2O_2 to be 75% scavenged (250 pptv). Horizontal lines represent the steady-state solution.

Table 4. Median Values for H_2O, NO, H_2O_2, CH_3OOH, H_2O_2(meas/calc), and CH_3OOH(meas/calc) for 8-12 km, 20°N-10°S During PEM-West B

	High NO_x	Low NO_x
H_2O, ppmv	178	666
NO, pptv	62.5	6.2
H_2O_2, pptv	160	480
CH_3OOH, pptv	87	481
H_2O_2(meas/calc)	0.77	0.93
CH_3OOH(meas/calc)	1.57	2.16

Although the above cited modeling results point toward the need to critically examine local photochemical trends in the peroxides, it must be noted that model predictions such as those in Table 4 also have shortcomings in that they assume photochemical equilibrium. In reality, it is quite likely that much of the tropical upper troposphere is perturbed with a frequency that precludes reaching a local steady state [*Prather and Jacob*, 1997]. Thus, evaluating the time evolution of peroxides following a convective event as they move toward photochemical equilibrium values can prove useful. This type of approach has been implemented in studies by *Jaeglé et al.* [1997] and *Cohan et al.* [1999]. Here, simulations are based on median conditions for the PWB low NO_x regime for two cases. In the first, CH_3OOH and CH_2O are assumed to be transported from the marine boundary layer undiluted (e.g., 1 ppbv and 200 pptv, respectively) and H_2O_2 is assumed to be totally scavenged. The second case is different in that H_2O_2 is assumed to be 75% scavenged (e.g., 250 pptv). Results are shown in Figure 7. The time evolution of these species is somewhat artificial in that no dilution due to mixing is assumed, but the results still give some indication of how peroxide levels might evolve due to local photochemistry. In both cases, enhancements in CH_3OOH above steady state decrease from a factor of 5 to a factor of 2 at the end of 2 days. After 3 days, H_2O_2 is slightly above or below its steady-state value depending on the case assumed. CH_2O behaves much as CH_3OOH. HO_2 is initially elevated by 35%. Over the first day, diurnal average HO_2 is elevated by 21% above steady state with the largest enhancement (45%) occurring at sunrise. By the second day, the diurnal average enhancement rapidly diminishes to less than 15%, although a sunrise enhancement of 32% is still present. OH is initially depressed by 20% with a recovery to within 10% of steady state within the first day.

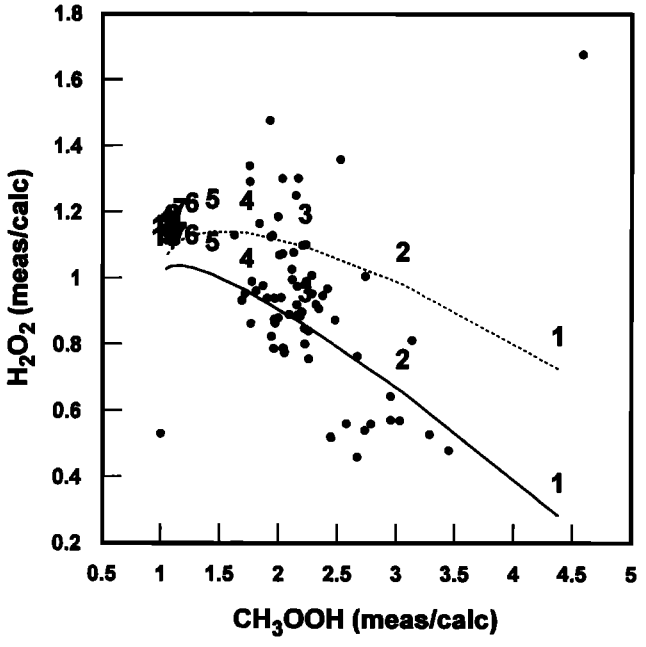

Figure 8. Scatterplot of H_2O_2(meas/calc) versus CH_3OOH(meas/calc) for the low NO_x regime of PEM-West B. Solid and dotted lines represent the deviations from steady state predicted in Figure 7. Numbers along each line represent the number of days from the initial perturbation.

These calculations show how rapidly photochemical equilibrium for peroxides can be reestablished in a high water vapor environment such as the PWB low NO_x regime. It also shows that one might expect recently convected air to exhibit enhanced CH_3OOH accompanied by depleted H_2O_2. Figure 8 examines the peroxide observations for the PWB low NO_x regime in terms of this expectation. While it is not realistic to expect the field data to closely match these simulations, it is interesting to see that when observations of CH_3OOH are elevated above their calculated steady-state values in this data, H_2O_2 observations tend to be depleted below their calculated steady-state values. Thus, there is some consistency in the measured-to-calculated peroxide ratios with the argument that they have been influenced by convection.

Recalling the sensitivity calculations, peroxides were estimated to have their greatest impact on HO_x levels at 11-12 km (~ 30%). One of the more interesting aspects of these results was finding that at this altitude the largest HO_x increase is related to the constraint of H_2O_2, not CH_3OOH. This was found to be true even though Figure 3 clearly shows that the ratio of measured-to-calculated values for CH_3OOH exhibit the largest increase above 8 km. This is suggestive of fast vertical transport, but it is also possible that this trend may be somewhat overestimated, especially for 11-12 km, owing to the large percentage of the CH_3OOH data at LOD values (i.e., 42%). In this context, the question can be raised whether the enhanced value of the ratio for H_2O_2 at 11-12 km is, in fact, understood. For example, if the observed H_2O_2 enhancement is to be attributed to convection, one could argue that there should be some correspondence with the enhancement in CH_3OOH. Looking specifically at the CH_3OOH observations at 11-12 km that were at or below LOD, it would seem difficult to argue that these CH_3OOH levels were significantly influenced by convection. Yet for this subset of data, the median ratio of measured-to-calculated H_2O_2 remains significantly greater than one (i.e., 3.6). This would seem to suggest that the enhancement in the H_2O_2 ratio at 11-12 km is not due to convection but rather to other factors such as local photochemistry.

Similar to the PWB low NO_x regime, Figure 9 examines the time evolution of convectively perturbed peroxides based on median conditions for all tropical PEM data at 11-12 km. The two perturbation scenarios used here are the same as those used for the PWB low NO_x regime model runs. The most significant difference between these two data sets is the water vapor mixing ratio. The 11-12 km data has a median value of 15 ppmv; whereas, the PWB low NO_x regime has a median of 600 ppmv. As shown in Figure 9, the time evolution profiles based on the 11-12 km data show some significant differences, especially with respect to H_2O_2. Both CH_3OOH and CH_2O decay rapidly over the first 2-3 days, although, CH_3OOH is still significantly above its steady-state value even after 3 days. H_2O_2 in this low H_2O environment is enhanced above the steady-state value by as much as 2-5 times, depending on the scenario. In agreement with the calculations of *Jaeglé et al.* [1997] and *Cohan et al.* [1999], the enhancement in H_2O_2 persists longer than that for CH_3OOH. Large initial enhancements in HO_2 and OH are also observed in these calculations. These enhancements relax to diurnal average values that are about 20% above final steady state after 3 days. These calculations demonstrate two important points: (1) in a low water vapor environment, H_2O_2 and CH_3OOH enhancements due to convection are not simultaneous and (2) enhanced H_2O_2 can continue to influence HO_x well after the perturbation in CH_3OOH levels has dissipated.

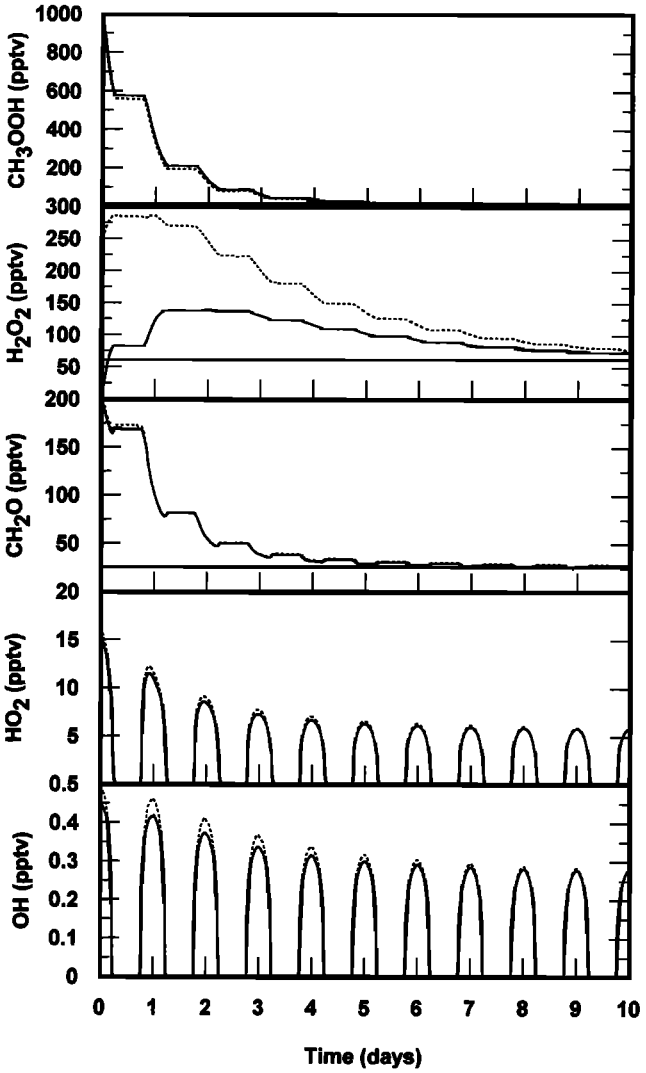

Figure 9. Time evolution of convectively perturbed peroxides and CH_2O for median conditions observed at 11-12 km. Perturbations consist of typical marine boundary layer values for CH_3OOH (1 ppbv) and CH_2O (200 pptv). Solid lines represent the assumption of total scavenging of H_2O_2. Dotted lines assume H_2O_2 to be 75% scavenged (250 pptv). Horizontal lines represent the steady-state solution.

While convection of peroxides is inarguably an important consideration in understanding upper tropospheric HO_x, it is important to recognize that the close relationship between HO_x and H_2O_2 possesses a certain level of ambiguity. Elevated H_2O_2 will lead to elevated HO_x, but the reverse is also true. Is it possible that the elevated H_2O_2 at 11-12 km is simply a reflection of elevated HO_x levels due to a source which is unaccounted for by any of the constraints considered here? Such possibilities are examined below.

6.3. Other Possible HO_x Influences?

During the STRAT campaign, HO_2 observations were found to exceed what might be expected from water vapor and acetone by a factor of 1.5 on average with instances of differences as high as a factor of 5 [*Jaeglé et al.*, 1997]. During SUCCESS, HO_x measurements were sometimes in agreement with predictions, while at other times they exceeded predictions by factors of 4 [*Brune et al.*, 1998]. In both studies, the possibility that convected peroxides might constitute an important additional source of HO_x was proposed. The results from the PEM data suggest that peroxides could have resulted in increases in HO_x, but even at 11-12 km the increase is typically no more than 30% and never more than a factor of 2. While the median increase of 30% does approach the mean increase of 1.5 cited for the STRAT data, recall that the additional 20% difference requires nontrivial increases in primary HO_x production.

In all likelihood, differences between these campaigns are most likely explained by the fact that conditions observed during the PEM missions were simply different from those encountered during STRAT and SUCCESS. In STRAT, for instance, the ER-2 sampled between altitudes of 8 km and the tropopause (15-17 km), while the DC-8 was limited to a ceiling of 12 km during the PEM missions. It is also noteworthy, however, that discrepancies between measured and calculated HO_x during STRAT were greatest for the lower altitudes (i.e, 10-12 km) with higher water vapor (i.e., 30-80 ppmv), while the drier air masses at higher altitudes appeared to be explainable in terms of water vapor and acetone only [*McKeen et al.*, 1997]. STRAT data highlighted by *Jaeglé et al.* [1997] was also predominantly in the 11-12 km altitude range. Regardless of the similarities and differences between these campaigns, it is worthwhile to explore the possibility that other still unidentified impacts on HO_x may exist.

One possibility for additional HO_x could come from the extension of known NMHC sources to include the presence of more complex, but analogous oxygenated hydrocarbons [*S. Liu et al.*, unpublished manuscript, 1999]. For instance, acetone could be extended to include all ketones. While higher-order ketones are expected to have much less abundance, they also might provide a greater yield of HO_x. The same can be said for organic peroxides, alcohols, and aldehydes. Although measuring all of these species is currently impractical, some indication of the importance of these sources could be gained through measurements of CH_2O. Recall, calculations showed CH_2O to be far more sensitive than either HO_x or CH_3O_2. Thus, measurements of this species in the upper troposphere could prove to be a useful indicator of the integrated impact from NMHC sources.

Another possible HO_x source proposed by *Toumi* [1993] also demands new attention in light of the recent HO_x observations. *Toumi* proposed that OH may be produced in the atmosphere by reaction of electronically excited oxygen with hydrogen (i.e., $O_2(b^1\Sigma_g) + H_2 \rightarrow 2OH$). While $O_2(b^1\Sigma_g)$ is expected to be collisionally quenched, *Toumi* showed that even if only 1% of the collisions result in a reaction, the resulting primary production of OH would exceed that for $O(^1D)+H_2O$ in the upper troposphere. In Toumi's study the potential importance of this reaction was maximized in the upper troposphere both due to the increasing abundance of $O_2(b^1\Sigma_g)$ and due to the decreasing amount of water vapor. In a follow-up study by *Siskind et al.* [1993], it was pointed out that after correcting for an overestimate by *Toumi* for the abundance of $O_2(b^1\Sigma_g)$, 4% of the collisions were required to be reactive to be equivalent to the original proposal by *Toumi*. *Siskind et al.* also noted that the resulting impact would increase the diurnal-average OH abundance by up to a factor of 2 at an altitude of 15 km.

Subsequent to these theoretical studies, no laboratory studies were initiated to support or refute the possible importance of this reaction. Recently, however, a laboratory study has been conducted which shows this reaction to have an OH yield of less

Table A1. Chemical Mechanism for the Photochemical Box Model

Reaction	Rate Coefficient	Notes
Basic HO_x-NO_x-CH_4 Reactions		
Gas Phase Reactions		
k_1 $O(^1D)+N_2 \rightarrow O(^3P)$	$1.8\times10^{-11}\exp(110/T)$	a
k_2 $O(^1D)+O_2 \rightarrow O(^3P)$	$3.2\times10^{-11}\exp(70/T)$	a
k_3 $O(^1D)+H_2O \rightarrow 2OH$	2.2×10^{-10}	a
k_4 $O(^1D)+CH_4 \rightarrow CH_3+OH$	1.35×10^{-10}	a
k_5 $O(^1D)+CH_4 \rightarrow CH_2O+H_2$	1.5×10^{-11}	a
k_6 $O(^1D)+H_2 \rightarrow H+OH$	1.1×10^{-10}	a
k_7 $OH+CO \rightarrow CO_2+H$	$1.5\times10^{-13}(1+0.6P_{atm})$	a
k_8 $H+O_2+M \rightarrow HO_2$	$k_o^{300}=5.7\times10^{-32}$, n=1.6, $k_\infty^{300}=7.5\times10^{-11}$, m=0	a,p
k_9 $HO_2+NO \rightarrow NO_2+OH$	$3.5\times10^{-12}\exp(250/T)$	a
k_{10} $HO_2+O_3 \rightarrow OH+2O_2$	$1.1\times10^{-14}\exp(-500/T)$	a
k_{11} $HO_2+HO_2 \rightarrow H_2O_2$	$[2.3\times10^{-13}\exp(600/T)+1.7\times10^{-33}[M]\exp(1000/T)]$ *$[1+1.4\times10^{-21}[H_2O]\exp(2200/T)]$	a
k_{12} $OH+HO_2 \rightarrow H_2O+O_2$	$4.8\times10^{-11}\exp(250/T)$	a
k_{13} $HO_2+NO_2+M \rightarrow HO_2NO_2$	$k_o^{300}=1.8\times10^{-31}$, n=3.2, $k_\infty^{300}=4.7\times10^{-12}$, m=1.4	a,p
k_{14} $HO_2NO_2+M \rightarrow HO_2+NO_2$	$k_{13}/(2.1\times10^{-27}\exp(10900/T))$	a
k_{15} $HO_2+NO_3 \rightarrow OH+NO_2+O_2$	3.5×10^{-12}	a
k_{16} $H_2O_2+OH \rightarrow HO_2+H_2O$	$2.9\times10^{-12}\exp(-160/T)$	a
k_{17} $CH_4+OH \rightarrow CH_3+H_2O$	$2.8\times10^{-14}\exp(-1575/T)*T^{0.667}$	a
k_{18} $CH_3+O_2+M \rightarrow CH_3O_2$	$k_o^{300}=4.5\times10^{-31}$, n=3, $k_\infty^{300}=1.8\times10^{-12}$, m=1.7	a,p
k_{19} $CH_3O_2+NO \rightarrow CH_3O+NO_2$	$3.0\times10^{-12}\exp(280/T)$	a
k_{20} $CH_3O_2+HO_2 \rightarrow CH_3OOH+O_2$	$3.8\times10^{-13}\exp(800/T)$	a
k_{21} $CH_3O_2+CH_3O_2 \rightarrow 2CH_3O+O_2$	$0.4*2.5\times10^{-13}\exp(190/T)$	a
k_{22} $CH_3O_2+CH_3O_2 \rightarrow CH_2O+CH_3OH$	$0.6*2.5\times10^{-13}\exp(190/T)$	a
k_{23} $CH_3O_2+NO_2+M \rightarrow CH_3O_2NO_2$	$k_o^{300}=1.5\times10^{-30}$, n=4, $k_\infty^{300}=6.5\times10^{-12}$, m=2	a,p
k_{24} $CH_3O_2NO_2+M \rightarrow CH_3O_2+NO_2$	$k_{23}/(1.3\times10^{-28}\exp(11200/T))$	a
k_{25} $CH_3OOH+OH \rightarrow CH_3O_2+H_2O$	$0.7*3.8\times10^{-12}\exp(200/T)$	a
k_{26} $CH_3OOH+OH \rightarrow CH_2O+OH+H_2O$	$0.3*3.8\times10^{-12}\exp(200/T)$	a
k_{27} $CH_2O+OH \rightarrow CHO+H_2O$	1.0×10^{-11}	a
k_{28} $CH_2O+NO_3 \rightarrow HNO_3+CHO$	5.8×10^{-16}	a
k_{29} $CH_3O+O_2 \rightarrow CH_2O+HO_2$	$3.9\times10^{-14}\exp(-900/T)$	a
k_{30} $CHO+O_2 \rightarrow HO_2+CO$	$3.5\times10^{-12}\exp(140/T)$	a
k_{31} $OH+CH_3OH \rightarrow CH_2OH+H_2O$	$6.7\times10^{-12}\exp(-600/T)$	a
k_{32} $CH_2OH+O_2 \rightarrow CH_2O+HO_2$	9.1×10^{-12}	a
k_{33} $OH+H_2 \rightarrow H_2O+H$	$5.5\times10^{-12}\exp(-2000/T)$	a
k_{34} $O_3+OH \rightarrow HO_2+O_2$	$1.6\times10^{-12}\exp(-940/T)$	a
k_{35} $O_3+NO \rightarrow NO_2+O_2$	$2.0\times10^{-12}\exp(-1400/T)$	a
k_{36} $O_3+NO_2 \rightarrow NO_3+O_2$	$1.2\times10^{-13}\exp(-2450/T)$	a
k_{37} $OH+NO+M \rightarrow HONO$	$k_o^{300}=7.0\times10^{-31}$, n=2.6, $k_\infty^{300}=3.6\times10^{-11}$, m=0.1	a,p
k_{38} $OH+NO_2+M \rightarrow HNO_3$	$k_o^{300}=2.5\times10^{-30}$, n=4.4, $k_\infty^{300}=1.6\times10^{-11}$, m=1.7	a,p
k_{39} $OH+NO_3 \rightarrow HO_2+NO_2$	2.2×10^{-11}	a
k_{02} $OH+HNO_3 \rightarrow H_2O+NO_3$	see note q	a
k_{41} $OH+HONO \rightarrow NO_2+H_2O$	$1.8\times10^{-11}\exp(-390/T)$	a
k_{42} $OH+HO_2NO_2 \rightarrow NO_2+H_2O+O_2$	$1.3\times10^{-12}\exp(380/T)$	a
k_{43} $NO_3+M \rightarrow NO+O_2$	$2.5\times10^{6}\exp(-6100/T)$	g
k_{44} $NO+NO_3 \rightarrow 2NO_2$	$1.5\times10^{-11}\exp(170/T)$	a
k_{45} $NO_3+CO \rightarrow NO_2+CO_2$	4.0×10^{-19}	a
k_{46} $NO_2+NO_3+M \rightarrow N_2O_5$	$k_o^{300}=2.2\times10^{-30}$, n=3.9, $k_\infty^{300}=1.5\times10^{-12}$, m=0.7	a,p
k_{47} $N_2O_5+M \rightarrow NO_2+NO_3$	$k_{46}/(2.7\times10^{-27}\exp(11000/T))$	a
k_{48} $N_2O_5+H_2O \rightarrow 2HNO_3$	2.0×10^{-21}	a
Rainout/Washout and Deposition		
R_1 H_2O_2,CH_3OOH,CH_2O,CH_3OH,HNO_3, HONO,HO_2NO_2 → Rainout/Washout	0-4 km, 2.31×10^{-6} > 4 km (z in km), $2.31\times10^{-6}\exp(1.6-0.4z)$	h
D_1 H_2O_2,CH_2O,CH_3OH,HNO_3,HONO, HO_2NO_2 → Surface Deposition	0-1 km, 1.0×10^{-5}; > 1 km, 0.0	i
D_2 CH_3OOH → Surface Deposition	0-1 km, 3.0×10^{-6}; > 1 km, 0.0	i
A_1 NO_3,N_2O_5 → Aerosol	$\gamma=0.1$	j
Photolytic Reactions		
J_1 $O_3+h\nu \rightarrow O(^1D)$	4.3×10^{-5}	a,k,o
J_2 $H_2O_2+h\nu \rightarrow 2OH$	7.4×10^{-6}	a,o
J_3 $CH_3OOH+h\nu \rightarrow CH_3O+OH$	5.4×10^{-6}	a,o
J_4 $CH_2O+h\nu \rightarrow CHO+H$	2.9×10^{-5}	a,o
J_5 $CH_2O+h\nu \rightarrow CO+H_2$	4.8×10^{-5}	a,o
J_6 $NO_2+h\nu \rightarrow NO+O$	9.0×10^{-3}	a,o
J_7 $NO_3+h\nu \rightarrow NO_2+O$	3.3×10^{-1}	b,o

Table A1. (continued)

Reaction	Rate Coefficient	Notes
J_8 $N_2O_5+h\nu \rightarrow NO_2+NO_3$	5.0×10^{-5}	a,o
J_9 $HNO_3+h\nu \rightarrow OH+NO_2$	7.5×10^{-7}	a,o
J_{10} $HO_2NO_2+h\nu \rightarrow HO_2+NO_2$	3.1×10^{-6}	a,o
J_{11} $HO_2NO_2+h\nu \rightarrow OH+NO_3$	1.5×10^{-6}	a,o
J_{12} $HONO+h\nu \rightarrow OH+NO$	1.9×10^{-3}	a,o
Nonmethane Hydrocarbon Reactions		
Ketones		
kK_1 $CH_3COCH_3+OH \rightarrow CH_3COCH_2O_2+H_2O$	$2.2\times10^{-12}\exp(-685/T)$	b
kK_2 $MEK+OH \rightarrow KO_2+H_2O$	$1.8\times10^{-11}\exp(-890/T)$	d
kK_3 $CH_3COCH_3+h\nu \rightarrow CH_3CO_3+CH_3O_2$	6.9×10^{-7}	l,o
kK_4 $MEK+h\nu \rightarrow CH_3CO_3+C_2H_5O_2$	$3.6\times10^{-4}J(NO_2)$	d
kK_5 $MEK+NO_3 \rightarrow KO_2+HNO_3$	7.0×10^{-16}	c
kK_6 $CH_3COCH_2O_2+NO \rightarrow 0.04RAN_2+0.96(NO_2+MGLY+HO_2)$	$2.6\times10^{-12}\exp(365/T)$	e
kK_7 $KO_2+NO \rightarrow 0.07RAN_2+0.93(NO_2+ALD_2+CH_3CO_3)$	$2.6\times10^{-12}\exp(365/T)$	e
kK_8 $CH_3COCH_2O_2+HO_2 \rightarrow CH_3CO_3+CH_3O_2+H_2O$	$7.5\times10^{-13}\exp(700/T)$	f
kK_9 $KO_2+HO_2 \rightarrow MGLY+CH_3O_2+H_2O$	$7.5\times10^{-13}\exp(700/T)$	f
Alkanes		
kA_1 $C_2H_6+OH \rightarrow C_2H_5O_2+H_2O$	$8.7\times10^{-12}\exp(-1070/T)$	a
kA_2 $C_2H_5O_2+NO \rightarrow ALD_2+HO_2+NO_2$	$2.6\times10^{-12}\exp(365/T)$	a
kA_3 $C_2H_5O_2+HO_2 \rightarrow C_2H_5OOH+O_2$	$7.5\times10^{-13}\exp(700/T)$	a
kA_4 $C_2H_5O_2+C_2H_5O_2 \rightarrow 1.6ALD_2+1.2HO_2$	6.8×10^{-14}	a
kA_5 $C_3H_8+OH \rightarrow n\text{-}C_3H_7O_2+H_2O$	$6.3\times10^{-12}\exp(-1050/T)$	a
kA_6 $C_3H_8+OH \rightarrow i\text{-}C_3H_7O_2+H_2O$	$6.3\times10^{-12}\exp(-580/T)$	a
kA_7 $n\text{-}C_3H_7O_2+NO \rightarrow ALD_2+NO_2+HO_2$	8.7×10^{-12}	b
kA_8 $i\text{-}C_3H_7O_2+NO \rightarrow CH_3COCH_3+NO_2+HO_2$	8.5×10^{-12}	b
kA_9 $n\text{-}C_3H_7O_2+HO_2 \rightarrow n\text{-}C_3H_7OOH+O_2$	$7.5\times10^{-13}\exp(700/T)$	f
kA_{10} $i\text{-}C_3H_7O_2+HO_2 \rightarrow i\text{-}C_3H_7OOH+O_2$	$7.5\times10^{-13}\exp(700/T)$	f
kA_{11} $n\text{-}C_3H_7O_2+n\text{-}C_3H_7O_2 \rightarrow 1.5ALD_2+0.5n\text{-}C_3H_7OH+HO_2$	3.0×10^{-13}	b
kA_{12} $i\text{-}C_3H_7O_2+i\text{-}C_3H_7O_2 \rightarrow 1.5CH_3COCH_3+0.5i\text{-}C_3H_7OH+HO_2$	$1.6\times10^{-12}\exp(-2200/T)$	b
kA_{13} $ALKA+OH \rightarrow RAO_2+H_2O$	$2.0\times10^{-11}\exp(-500/T)$	c
kA_{14} $ALKA+NO_3 \rightarrow RAO_2+HNO_3$	4.0×10^{-17}	c
kA_{15} $RAO_2+NO \rightarrow ß_1NO_2+ß_2NO+ß_3RAN_2+ß_4ALD_2+ß_5MEK+ß_6C_2H_5O_2+ß_7CH_3O_2+ß_8HO_2+ß_9C_3H_7O_2+0.06RAO_2$	$2.6\times10^{-12}\exp(365/T)$	e, ß
kA_{16} $RAO_2+HO_2 \rightarrow RAP+O_2$	$7.5\times10^{-13}\exp(700/T)$	f
kA_{17} $RAN_2+OH \rightarrow RAN_1+H_2O$	2.0×10^{-12}	c
kA_{18} $RAN_1+NO \rightarrow NO_2+HCHO+RANO_2$	$2.6\times10^{-12}\exp(365/T)$	e
kA_{19} $RAN_1/RANO_2+HO_2 \rightarrow RANP/RANP_2$	$7.5\times10^{-13}\exp(700/T)$	f
kA_{20} $RANO_2+NO \rightarrow 2NO_2+2ALD_2$	$2.6\times10^{-12}\exp(365/T)$	e
Alkenes		
kE_1 $C_2H_4+OH \rightarrow HOC_2H_3O_2$	$k_o^{300}=1.0\times10^{-28}$, n=0.8 $k_\infty^{300}=8.8\times10^{-12}$, m=0	a,p
kE_2 $C_2H_4+O_3 \rightarrow HCHO+0.4CHO_2+0.12HO_2+0.42CO+0.06CH_4$	$1.2\times10^{-14}\exp(-2633/T)$	c
kE_3 $HOC_2H_3O_2+NO \rightarrow NO_2+2HCHO+HO_2$	$2.6\times10^{-13}\exp(365/T)$	e
kE_4 $HOC_2H_3O_2+HO_2 \rightarrow HOC_2H_3OOH+O_2$	$7.5\times10^{-13}\exp(700/T)$	f
kE_5 $HOC_2H_3O_2+HOC_2H_3O_2 \rightarrow 2.4HCHO+1.2HO_2+0.4ALD_2$	5.0×10^{-14}	c
kE_6 $ALKE+OH \rightarrow PO_2$	$4.1\times10^{-12}\exp(537/T)$	c
kE_7 $ALKE+O_3 \rightarrow 0.525HCHO+0.5ALD_2+0.2(CHO_2+CRO_2)+0.23HO_2+0.215CH_3O_2+0.095OH+0.33CO$	$7.8\times10^{-14}\exp(-2105/T)$	c
kE_8 $ALKE+NO_3 \rightarrow PRN_1$	1.26×10^{-13}	c
kE_9 $PO_2+NO \rightarrow NO_2+ALD_2+HCHO+HO_2$	$2.6\times10^{-13}\exp(365/T)$	e
kE_{10} $PO_2+HO_2 \rightarrow PP+O_2$	$7.5\times10^{-13}\exp(700/T)$	f
kE_{11} $PO_2+PO_2 \rightarrow 2.2ALD_2+1.2HO_2$	5.0×10^{-14}	c
kE_{12} $PRN_1+NO_2 \rightarrow PRN_2$	6.8×10^{-12}	c
kE_{13} $PRN_1+HO_2 \rightarrow PRPN+O_2$	$7.5\times10^{-13}\exp(700/T)$	f
kE_{14} $PRN_1+NO \rightarrow 2NO_2+HCHO+ALD_2$	$2.6\times10^{-13}\exp(365/T)$	e
kE_{15} $CHO_2+NO \rightarrow HCHO+NO_2$	7.0×10^{-12}	c
kE_{16} $CHO_2+NO_2 \rightarrow HCHO+NO_3$	7.0×10^{-13}	c
kE_{17} $CHO_2+H_2O \rightarrow HCOOH$	4.0×10^{-18}	c
kE_{18} $CHO_2+SO_2 \rightarrow HCHO+SO_4$	7.0×10^{-14}	c
kE_{19} $CHO_2+HCHO \rightarrow OZID$	1.36×10^{-14}	c
kE_{20} $CHO_2+ALD_2 \rightarrow OZID$	1.36×10^{-14}	c
kE_{21} $CRO_2+NO \rightarrow ALD_2+NO_2$	7.0×10^{-12}	c
kE_{22} $CRO_2+NO_2 \rightarrow ALD_2+NO_3$	7.0×10^{-13}	c
kE_{23} $CRO_2+H_2O \rightarrow CH_3COOH$	4.0×10^{-18}	c
kE_{24} $CRO_2+SO_2 \rightarrow ALD_2+SO_4$	7.0×10^{-14}	c
kE_{25} $CRO_2+HCHO \rightarrow OZID$	1.36×10^{-14}	c
kE_{26} $CRO_2+ALD_2 \rightarrow OZID$	1.36×10^{-14}	c

Table A1. (continued)

Reaction	Rate Coefficient	Notes
Isoprene		
kI_1 ISOP+OH→RIO_2	4.0×10^{-10}exp(-410/T)	m
kI_2 ISOP+O_3→0.5HCHO+0.2MVK+0.3MACR+0.2CHO_2+0.06HO_2+0.2MVKO+0.3MAOO	7.0×10^{-15}exp(-1900/T)	d
kI_3 ISOP+NO_3→INO_2	3.23×10^{-13}	d
kI_4 RIO_2+NO→0.9(NO_2+HO_2+HCHO)+0.45(MVK+MACR)	2.6×10^{-12}exp(365/T)	e
kI_5 RIO_2+HO_2→XAP_1+O_2	7.5×10^{-13}exp(700/T)	f
kI_6 INO_2+NO→2NO_2+HCHO+0.5(MVK+MACR)	2.6×10^{-12}exp(365/T)	e
kI_7 INO_2+NO_2→IPN_4	0.1kP_6	d
kI_8 INO_2+HO_2→PROD	7.5×10^{-13}exp(700/T)	f
kI_9 MVK+OH→VRO_2	0.2 kP_1	d
kI_{10} MVK+O_3→0.5(MGGY+HCHO)+0.2(CHO_2+CRO_2)+0.21HO_2+0.15ALD_2+0.15CH_3CO_3	4.0×10^{-15}exp(-2000/T)	d
kI_{11} MVK+NO_3→MVN_2	6.0×10^{-14}	d
kI_{12} VRO_2+NO→0.9NO_2+0.6(CH_3CO_3+ALD_2)+0.3(HO_2+HCHO+MGLY)	2.6×10^{-12}exp(365/T)	e
kI_{13} VRO_2+HO_2→RP+O_2	7.5×10^{-13}exp(700/T)	f
kI_{14} MVN_2+NO→2NO_2+HCHO+0.5(CH_3CO_3+MGGY+HO_2)	2.6×10^{-12}exp(365/T)	e
kI_{15} MVN_2+HO_2→PROD	7.5×10^{-13}exp(700/T)	f
kI_{16} MACR+OH→MAO_3	1.02×10^{-11}	d
kI_{17} MACR+OH→MRO_2	3.86×10^{-12}exp(500/T)	d
kI_{18} MACR+O_3→0.65HCHO+0.5MGGY+0.36HO_2+0.2(CHO_2+CRO_2)+0.15(NO_2-NO)	4.4×10^{-15}exp(-2500/T)	d
kI_{19} MACR+NO_3→MAO_3+HNO_3	3.3×10^{-15}	d
kI_{20} MACR+NO_3→MAN_2	6.7×10^{-15}	d
kI_{21} MAO_3+NO_2→MPAN	4.7×10^{-12}	d
kI_{22} MPAN→MAO_3+NO_2	1.95×10^{16}exp(-13543/T)	d
kI_{23} MAO_3+NO→NO_2+PO_2+CO_2	2.6×10^{-12}exp(365/T)	e, n
kI_{24} MAO_3+HO_2→DAP+O_2	7.5×10^{-13}exp(700/T)	f
kI_{25} MRO_2+NO→0.9(NO_2+HO_2+CO+HACO)	2.6×10^{-12}exp(365/T)	e, n
kI_{26} MRO_2+HO_2→XAP_2+O_2	7.5×10^{-13}exp(700/T)	f
kI_{27} MAN_2+NO→2NO_2+HCHO+MGGY	2.6×10^{-12}exp(365/T)	e
kI_{28} MAN_2+HO_2→PROD	7.5×10^{-13}exp(700/T)	f
kI_{29} MVKO+NO→MVK+NO_2	2.6×10^{-12}exp(365/T)	e
kI_{30} MVKO+NO_2→MVK+NO_3	0.1kP_{29}	d
kI_{31} MVKO+H_2O→PROD	3.4×10^{-18}	d
kI_{32} MVKO+HO_2→PROD	7.5×10^{-13}exp(700/T)	f
kI_{33} MVKO+SO_2→MVK+SO_4	7.0×10^{-14}	d
kI_{34} MAOO+NO→MACR+NO_2	2.6×10^{-12}exp(365/T)	e
kI_{35} MAOO+NO_2→MACR+NO_3	0.1kP_{34}	d
kI_{36} MAOO+H_2O→PROD	3.4×10^{-18}	d
kI_{37} MAOO+HO_2→PROD	7.5×10^{-13}exp(700/T)	f
kI_{38} MAOO+SO_2→MACR+SO_4	7.0×10^{-14}	d
kI_{39} MGGY+hν→CH_3CO_3+HO_2	0.15 J(NO_2)	d
kI_{40} MGGY+OH→CH_3CO_3	1.7×10^{-11}	d
Aromatics		
kM_1 C_6H_6+OH→C_6H_6(OH)OO	1.2×10^{-12}	d
kM_2 C_6H_6(OH)OO+NO→NO_2+HO_2+GLYX+DIAL	2.6×10^{-13}exp(365/T)	e
kM_3 AROM+OH→0.84TO_2+0.16CRES+0.16HO_2	1.52×10^{-11}	c
kM_4 TO_2+NO→NO_2+HO_2+0.72MGLY+0.18GLYX+DIAL	2.6×10^{-13}exp(365/T)	e
kM_5 TO_2+HO_2→TP+O_2	4.0×10^{-12}	c
kM_6 CRES+OH→$ß_{12}$HO2+0.9(ZO_2+TCO_3-OH)+$ß_{13}NO_2$	4.25×10^{-11}	c, β
kM_7 CRES+NO_3→HNO_3+$ß_{10}$NO2+$ß_{11}$OH	1.0×10^{-11}	c, β
kM_8 MGLY+hν→CH_3CO_3+HO_2+CO	0.019 J(NO_2)	c
kM_9 MGLY+OH→CH_3CO_3+H_2O+CO	1.73×10^{-11}	c
kM_{10} GLYX+hν→PROD	0.008 J(NO_2)	c
kM_{11} GLYX+OH→HO_2+2CO+H_2O	1.15×10^{-11}	c
kM_{12} DIAL+hν→0.98HO_2+0.02CH_3CO_3+TCO_3	0.01 J(NO_2)	c
kM_{13} DIAL+OH→TCO_3+H_2O	2.8×10^{-11}	c
kM_{14} ZO_2+NO→NO_2	2.6×10^{-13}exp(365/T)	e
kM_{15} ZO_2+HO_2→ZP +O_2	1.0×10^{-12}	c
kM_{16} TCO_3+NO→NO_2+0.92HO_2+0.89GLYX+0.11MGLY+0.05CH_3CO_3+0.95CO+0.79CO_2+2ZO_2	2.6×10^{-13}exp(365/T)	e
kM_{17} TCO_3+HO_2→TCP+O_2	4.0×10^{-12}	c
kM_{18} TCO_3+NO_2→TPAN	4.7×10^{-12}	c
kM_{19} TPAN→TCO_3+NO_2	1.95×10^{16}exp(-13543/T)	c

Table A1. (continued)

Reaction	Rate Coefficient	Notes
Aldehydes		
kD_1 $ALD_2+OH \rightarrow CH_3CO_3+H_2O$	$5.6\times10^{-12}\exp(270/T)$	a
kD_2 $ALD_2+NO_3 \rightarrow CH_3CO_3+HNO_3$	$1.4\times10^{-12}\exp(-1900/T)$	a
kD_3 $ALD_2+h\nu \rightarrow CH_3O_2+HO_2+CO$	5.6×10^{-6}	b,o
kD_4 $ALD_2+h\nu \rightarrow CH_4+CO$	6.0×10^{-11}	b,o
kD_5 $CH_3CO_3+NO \rightarrow CH_3O_2+NO_2+CO_2$	$5.3\times10^{-12}\exp(360/T)$	a
kD_6 $CH_3CO_3+HO_2 \rightarrow 0.33(CH_3C(O)OOH+O_2)+0.67(CH_3COOH+O_3)$	$4.5\times10^{-13}\exp(1000/T)$	a
kD_7 $CH_3CO_3+NO_2 \rightarrow PAN$	$k_o^{300}=9.7\times10^{-29}$, n=5.6, $k_\infty^{300}=9.3\times10^{-12}$, m=1.5	a,p
kD_8 $PAN \rightarrow CH_3CO_3+NO_2$	$kD_7/(9.0\times10^{-29}\exp(14000/T))$	a
kD_9 $CH_3CO_3+CH_3O_2 \rightarrow CH_3C(O)OH+CH_2O+O_2$	$1.3\times10^{-12}\exp(640/T)(1+2.2\times10^{6}\exp(-3820/T))$	a
kD_{10} $CH_3CO_3+CH_3O_2 \rightarrow CH_3O_2+CH_2O+HO_2+CO_2$	$1.3\times10^{-12}\exp(640/T)(1+1/(2.2\times10^{6}\exp(-3820/T)))$	a
kD_{11} $PAN+OH \rightarrow 0.5\ NO_2+$products	4.0×10^{-14}	a
kD_{12} $PAN+h\nu \rightarrow CH_3CO_3+NO_2$	8.6×10^{-7}	a
Organic Acids and Alcohols		
kC_1 $HCOOH+OH \rightarrow HO_2+CO_2+H_2O$	4.0×10^{-13}	a
kC_2 $CH_3COOH+OH \rightarrow CH_3O_2+CO_2+H_2O$	$4.0\times10^{-13}\exp(200/T)$	a
kC_3 $C_2H_5OH+OH \rightarrow ALD_2+HO_2+H_2O$	$7.0\times10^{-12}\exp(-235/T)$	a
kC_4 $HCOOH,CH_3COOH,C_2H_5OH \rightarrow$ Rainout/Washout	0-4 km, 2.31×10^{-6} > 4 km (z in km), $2.31\times10^{-6}\exp(1.6-0.4z)$	h
Organic Peroxide Loss and Recycling		
kP_1 $C_2H_5OOH+OH \rightarrow 0.5(C_2H_5O_2+ALD_2+OH)+H_2O$	1.0×10^{-11}	d
kP_2 $C_2H_5OOH+h\nu \rightarrow OH+HO_2+ALD_2$	$5.0\times10^{-4}J(NO_2)$	d
kP_3 $(n/i)C_3H_7OOH+OH \rightarrow 0.5(n/i\text{-}C_3H_7O_2+ALD_2+OH)+H_2O$	1.0×10^{-11}	d
kP_4 $(n/i)C_3H_7OOH+h\nu \rightarrow OH+HO_2+ALD_2$	$5.0\times10^{-4}J(NO_2)$	d
kP_5 $RAP+OH \rightarrow 0.5(RAO_2+ALD_2+OH)+H_2O$	$1\ 0\times10^{-11}$	d
kP_6 $RAP+h\nu \rightarrow OH+HO_2+ALD_2$	$5.0\times10^{-4}J(NO_2)$	d
kP_7 $CH_3C(O)OOH+OH \rightarrow 0.5(CH_3CO_3+HCHO+OH)+H_2O$	1.0×10^{-11}	d
kP_8 $CH_3C(O)OOH+h\nu \rightarrow OH+HO_2+HCHO$	$5.0\times10^{-4}J(NO_2)$	d
kP_9 $HOC_2H_3OOH+OH \rightarrow 0.5(HOC_2H_3O_2+2HCHO+OH)+H_2O$	1.0×10^{-11}	d
kP_{10} $HOC_2H_3OOH+h\nu \rightarrow OH+HO_2+2HCHO$	$5.0\times10^{-4}J(NO_2)$	d
kP_{11} $PP+OH \rightarrow 0.5(PO_2+ALD_2+OH)+H_2O$	1.0×10^{-11}	d
kP_{12} $PP+h\nu \rightarrow OH+HO_2+ALD_2$	$5.0\times10^{-4}J(NO_2)$	d
kP_{13} $TP+OH \rightarrow TO_2+H2O$	1.0×10^{-11}	d
kP_{14} $TCP+OH \rightarrow TCO_3+H2O$	1.0×10^{-11}	d
kP_{15} $ZP+OH \rightarrow ZO_2+H_2O$	1.0×10^{-11}	d
kP_{16} $XAP_1+OH \rightarrow 0.5(RIO_2+ALD_2+OH)+H_2O$	1.0×10^{-11}	d
kP_{17} $XAP_1+h\nu \rightarrow OH+HO_2+ALD_2$	$1.0\times10^{-3}J(NO_2)$	d
kP_{18} $RP+OH \rightarrow 0.5(VRO_2+ALD_2+OH)+H_2O$	1.0×10^{-11}	d
kP_{19} $RP+h\nu \rightarrow OH+HO_2+ALD_2$	$5.0\times10^{-4}J(NO_2)$	d
kP_{20} $DAP+OH \rightarrow 0.5(MAO_3+ALD_2+OH)+H_2O$	1.0×10^{-11}	d
kP_{21} $DAP+h\nu \rightarrow OH+HO_2+ALD_2$	$1.0\times10^{-3}J(NO_2)$	d
kP_{22} $XAP_2+OH \rightarrow 0.5(MRO_2+ALD_2+OH)+H_2O$	1.0×10^{-11}	d
kP_{23} $XAP_2+h\nu \rightarrow OH+HO_2+ALD_2$	$1.0\times10^{-3}J(NO_2)$	d
kP_{24} $HACO+NO_2 \rightarrow IPAN$	4.7×10^{-12}	d
kP_{25} $IPAN \rightarrow HACO+NO_2$	$1\ 95\times10^{16}\exp(-13543/T)$	d
kP_{26} $HACO+NO \rightarrow NO_2+HO_2+HCHO$	$2.6\times10^{-12}\exp(365/T)$	e
kP_{27} $HACO+HO_2 \rightarrow HEP$	3.0×10^{-12}	d
kP_{28} $HEP+OH \rightarrow 0.5(HACO+2HCHO+OH)+H_2O$	1.0×10^{-11}	d
kP_{29} $HEP+h\nu \rightarrow OH+HO_2+2HCHO$	$5.0\times10^{-4}J(NO_2)$	d
kP_{30} $C_2H_5OOH,(n/i)C_3H_7OOH,CH_3C(O)OOH,$ $HOC_2H_3OOH,DAP,HEP,PP,RAP,RP,TCP,$ $TP,XAP_1,XAP_2,ZP \rightarrow$ Rainout/Washout	0-4 km, 2.31×10^{-6} > 4 km (z in km), $2.31\times10^{-6}\exp(1.6-0.4z)$	h

[a] *DeMore et al.* [1997].
[b] *Atkinson et al.* [1992].
[c] Condensed chemical reaction mechanism [*Lurmann et al.*, 1986].
[d] Detailed chemical reaction mechanism [*Lurmann et al.*, 1986].
[e] Assumes rate for $C_2H_5O_2$ + NO.
[f] Assumes rate for $C_2H_5O_2$ + HO_2.
[g] *Johnston et al.* [1986].
[h] *Logan et al.* [1981].
[i] Estimated.
[j] *Dentener and Crutzen* [1993].
[k] Temperature dependence of cross section from *Molina and Molina* [1986] and quantum yields from *Talukdar et al.* [1998].
[l] Cross sections from *Hynes et al.* [1992] and quantum yields from *McKeen et al.* [1997].
[m] *Paulson et al.* [1992].
[n] Products based on *Paulson et al.* [1992].

[o]J values shown are calculated for the surface at 30° solar zenith angle, T = 298K, and an O_3 column density of 250 Dobson Units.
[p]Termolecular k values given by

$$k=\left(\frac{k_o(T)[M]}{1+(k_o(T)[M]/k_\infty(T))}\right)0.6^{[1+(\log_{10}(k_o(T)[M]/k_\infty(T)))^2]^{-1}}$$

where, $k_o(T)=k_o^{300}(T/300)^{-n}$ and $k_\infty(T)=k_\infty^{300}(T/300)^{-m}$
[q]Rate is given by

$$k=k_o+\frac{k_3[M]}{1+k_3[M]/k_2}$$

where, $k_o=7.2\times10^{-15}\exp(785/T)$, $k_2=4.1\times10^{-16}\exp(1440/T)$, and $k_3=1.9\times10^{-33}\exp(725/T)$
[β]Details on the calculation of β coefficients are found in *Lurmann et al.* [1986].

than 0.1% (R. K. Talukdar and A. R. Ravishankara, private communication, 1999). This result indicates that this reaction has no significant impact on diurnal average HO_x concentrations. Furthermore, this yield is too small to even expect any significant contribution at high solar zenith angles.

Finally, errors in kinetic rate coefficients and in OH calibration sources must be recognized as potential contributors to the discrepancy between observed and calculated HO_x levels. Errors in kinetic rate coefficients have been investigated previously through Monte Carlo calculations [*Thompson and Stewart*, 1991; *Thompson et al.*, 1997; *Davis et al.*, 1993; *Crawford et al.*, 1997b; *Crawford*, 1997]. In the upper troposphere, where temperatures are coldest, the uncertainties in calculated OH and HO_2 can become quite large (e.g. , 30-50%). The absolute calibration of OH instruments must also continue to be investigated for possible sources of systematic error. A major developement on this front would involve a rigorous (e.g., double blind) intercomparison of current airborne instruments. At present there appear to be at least two OH instruments (e.g., LIF and CIMS), based on totally different operating principles, that could be intercompared.

7. Summary

Data recorded in the tropical upper troposphere (8-12 km, 20°N-20°S) during NASA's Pacific Exploratory Missions (PEM-West A, PEM-West B, and PEM-Tropics A) have been used to examine HO_x photochemistry in this region. The availability of measurements of oxygenated hydrocarbons and peroxides from these flight campaigns have made it possible to quantitatively assess the potential impact from these species on HO_x levels as well as on other related photochemical parameters. Sensitivity calculations using a time dependent photochemical box model were carried out in which model runs were sequentially constrained by observations of water vapor, NMHCs, acetone, methanol/ethanol, CH_3OOH, and H_2O_2.

The impact due to constraining species was found to increase with altitude, reflecting the systematic roll-off in water vapor. Relative to water vapor chemistry which defined the base calculation, the largest increases below 11 km were associated with acetone and CH_3OOH. At 11-12 km, H_2O_2 contributed more to HO_x increases than CH_3OOH. The overall median increase in HO_x from all constraints approached a factor of 2 at

Table A2. Species Abbreviations Used in Nonmethane Hydrocarbon Reactions.

Abbr.	Definition	Abbr.	Definition
ALD_2	≥ C_2 aldehydes	MVN_2	MVK+NO_3 radical product
ALKA	lumped ≥ C_4 alkanes	OZID	ozonide or rearrangement product
ALKE	≥ C_3 alkenes	PAN	$CH_3CO_3NO_2$
AROM	aromatics	PO_2	≥ C_3 alkene RO_2
CHO_2	Criegee biradical (CH_2O_2)	PP	≥ C_3 alkene ROOH
CRES	Cresol	PRN_1	≥ C_3 alkene+NO_3 radical
CRO_2	Criegee biradical (CH_3CHO_2)	PRN_2	PRN_1+NO_2 radical
DAP	CH_2=C(CH_3)C(O)OOH	PROD	Undefined products
DIAL	unsaturated dicarbonyl	PRPN	PRN_1+HO_2 product
GLYX	$(CHO)_2$ (glyoxal)	RAN_1	≥ C_4 alkane RNO_2
HACO	$HOCH_2C(O)OO$	RAN_2	≥ C_4 alkane $RONO_2$
HEP	$HOCH_2C(O)OOH$	$RANO_2$	RAN_1+NO product
INO_2	isoprene-NO_3-O_2 adduct	RANP	RAN_1 ROOH
IPAN	$HOCH_2C(O)OONO_2$	$RANP_2$	$RANO_2$ ROOH
IPN_4	INO_2+NO_2 product	RAO_2	≥ C_4 alkane RO_2
ISOP	isoprene (C_5H_{10})	RAP	≥ C_4 alkane ROOH
KO_2	methyl ethyl ketone RO_2	RIO_2	isoprene RO_2
MACR	methacrolein	RP	RC(O)OOH (R=2)
MAN_2	MACR+NO_3 radical product	TCO_3	CHOCH=$CHCO_3$
MAO_3	CH_2=C(CH_3)C(O)OO	TCP	CHOCH=CHC(O)OOH
MAOO	Criegee biradical (CH_2=C(CH_3)CHOO)	TO_2	aromatic RO_2
MEK	methyl ethyl ketone ($CH_3COCH_2CH_3$)	TP	aromatic ROOH
MGGY	α-dicarbonyl	TPAN	CHOCH=$CHCO_3NO_2$
MGLY	CH_3COCHO (methylglyoxal)	VRO_2	MVK RO_2
MPAN	CH_2=C(CH_3)C(O)ONO_2	XAP_1	ISOP ROOH
MRO_2	MACR RO_2	XAP_2	MACR ROOH
MVK	methyl vinyl ketone	ZO_2	aromatic RO_2
MVKO	Criegee biradical (CH_2=CHC(OO)CH_3)	ZP	aromatic ROOH

11-12 km. Median increases in CH_3O_2 and CH_2O at 11-12 km exceeded a factor of 3, and increases in gross and net photochemical production of ozone exceeded a factor of 2.

An examination of the uncertainty in high-altitude water vapor revealed that calculations were fairly insensitive to large changes in water vapor (e.g., factors of 3-5) when absolute water vapor was below 100 ppmv. For fully constrained calculations (case F), the above cited differences in water vapor resulted in only a 5% change in HO_x levels. This result suggests that measurements of acetone and peroxides should be regarded as more critical than the accuracy of water vapor when the latter has mixing ratios below 100 ppmv. This lack of sensitivity to water below 100 ppmv is due both to the fact that water is no longer the dominant primary HO_x source and that secondary HO_x formation exceeds primary formation.

Peroxide observations were evaluated for evidence of convective impacts. For high water vapor environments such as the PWB low NO_x regime, calculations indicate that convectively perturbed peroxides rapidly return to expected steady-state values. The peroxide observations also support the contention that H_2O_2 is depleted relative to predicted steady-state values while CH_3OOH is elevated. In contrast, calculations based on the low water vapor environment at 11-12 km show that perturbations to CH_3OOH can lead to elevated H_2O_2 levels which can remain above the expected steady-state level for several days after CH_3OOH has dissipated. This potentially serves to explain why H_2O_2 can have values elevated above steady state by factors of 3 even when CH_3OOH is measured at or below its LOD.

The possibility that additional HO_x sources might be present in the upper troposphere was also explored. One suggestion hypothesized a potentially large integrated source of HO_x from the degradation of all organic peroxides/ketones/alcohols/aldehydes/etc. A second possibility relating to the reaction of $O_2(b^1\Sigma_g)$ with H_2 appears to be unimportant based on a recent laboratory study. Still other areas requiring continued investigation include further studies of temperature dependencies for gas kinetic rate coefficients at the low temperatures of the upper troposphere and further calibration exercises involving OH sensors. Both of these areas must be acknowledged as potential contributors to future disagreements between model calculations and observations.

Finally, it is recognized that as additional HO_x measurements are made in the upper troposphere, concurrent measurements of acetone and peroxides will be critical to establishing whether they alone are sufficient to explain the HO_x observations. In this context, measurements of CH_2O would also be of great value as a further indicator for sources of HO_x from a wide range of oxygenated hydrocarbon species.

Appendix

Table A1 provides a detailed list of the photochemical box model mechanism used in this study. Table A2 provides definitions for the numerous abbreviations used for NMHC-related species. Most of these abbreviations are in keeping with those established by *Lurmann et al.* [1986].

Acknowledgments. This work was supported by funds from NASA as part of the PEM-Tropics program. We would like to especially thank A. R. Ravishankara for his cooperation and timely laboratory results. We also thank two anonymous reviewers for their helpful comments.

References

Atkinson, R., D. L. Baulch, R. A. Cox, R. F. Hampson Jr., J. A. Kerr, and J. Troe, Evaluated kinetic and photochemical data for atmospheric chemistry, Supplement IV, IUPAC subcommittee on gas kinetic data evaluation for atmospheric chemistry, *J. Phys. Chem. Ref. Data, 21*, 1125-1568, 1992.

Bradshaw, J., et al., Photofragmentation two-photon laser-induced fluorescence detection of NO_2 and NO: Comparison of measurements with model results based on airborne observations during PEM-Tropics A, *Geophys. Res. Lett., 26*, 471-474, 1999.

Brasseur, G. P., J.-F. Müller, and C. Granier, Atmospheric impact of NO_x emissions by subsonic aircraft: A three-dimensional model study, *J. Geophys. Res., 101*, 1423-1428, 1996.

Brune, W H., et al., Airborne in situ OH and HO_2 observations in the cloud-free troposphere and stratosphere during SUCCESS, *Geophys. Res. Lett., 25*, 1701-1704, 1998.

Busen, R., and A. L. Buck, A high-performance hygrometer for aircraft use: Description, installation, and flight data, *J. Atmos. Oceanic Technol., 12*, 73-84, 1995.

Chatfield, R. B., and P. J. Crutzen, Sulfur dioxide in remote oceanic air: Cloud transport of reactive precursors, *J. Geophys. Res., 89*, 7111-7132, 1984.

Cohan, D. S., M. G. Schultz, D. J. Jacob, B. G. Heikes, and D. R. Blake, Convective injection and photochemical decay of peroxides in the upper troposphere, *J. Geophys. Res., 106*, 5717-5724, 1999.

Crawford, J. H., An analysis of the photochemical environment over the western, North Pacific based on airborne field observations, Ph.D. dissertation, Ga. Inst. of Technol., Atlanta, 1997.

Crawford, J., et al., Photostationary state analysis of the NO_2-NO system based on airborne observations from the western and central North Pacific, *J. Geophys. Res., 101*, 2053-2072, 1996.

Crawford, J., et al., Implications of large scale shifts in tropospheric NO_x levels in the remote tropical Pacific, *J. Geophys. Res., 102*, 28,447-28,468, 1997a.

Crawford, J. H., et al., An assessment of ozone photochemistry in the extratropical western North Pacific: Impact of continental outflow during the late winter/earlier spring, *J. Geophys. Res., 102*, 28,469-28,487, 1997b.

Crawford, J., D. Davis, G. Chen, R. Shetter, M. Müller, J. Barrick, and J. Olson, An assessment of cloud effects on photolysis rate coefficients: Comparison of experimental and theoretical values, *J. Geophys. Res., 104*, 5725-5734, 1999.

Davis, D. D., et al., Photostationary state analysis of the NO_2-NO system based on airborne observations from the subtropical/tropical North and South Atlantic, *J. Geophys. Res., 98*, 23,501-23,523, 1993.

Davis, D. D., et al., Assessment of the ozone photochemistry tendency in the western North Pacific as inferred from PEM-West A observations during the fall of 1991, *J. Geophys. Res., 101*, 2111-2134, 1996.

DeMore, W. B., S. P. Sander, D. M. Golden, R. F. Hampson, M. J. Kurylo, C. J. Howard, A. R. Ravishankara, C. E. Kolb, and M J. Molina, Chemical kinetics and photochemical data for use in stratospheric modeling, *JPL Publ., 97-4*, 1997.

Dentener, F. J., and P. J. Crutzen, Reaction of N_2O_5 on tropospheric aerosols: Impact on the global distributions of NO_x, O_3, and OH, *J. Geophys. Res., 98*, 7149-7163, 1993

Dickerson, R. R., et al., Thunderstorms: An important mechanism in the transport of air pollutants, *Science, 235*, 460-465, 1987.

Fishman, J., S. Solomon, and P. Crutzen, Observational and theoretical evidence in support of a significant in-situ photochemical source of tropospheric ozone, *Tellus, 31*, 432-446, 1979.

Folkins, I., R. Chatfield, H. Singh, Y. Chen, and B. Heikes, Ozone production efficiencies of acetone and peroxides in the upper troposphere, *Geophys. Res. Lett., 25*, 1305-1308, 1998.

Goldan, P. D., W. C. Kuster, F. C. Fehsenfeld, and S. A. Montzka, Hydrocarbon measurements in the southeastern United States: The rural oxidants in the southern environment (ROSE) program 1990, *J. Geophys. Res., 100*, 25,945-25,963, 1995.

Heikes, B. G., et al., Hydrogen peroxide and methylhydroperoxide distributions related to ozone and odd hydrogen over the North Pacific in the fall of 1991, *J. Geophys. Res., 101*, 1891-1905, 1996.

Hoell, J. M., D. D. Davis, S. C. Liu, R. Newell, M. Shipham, H. Akimoto, R. J. McNeal, R. J. Bendura, and J. W. Drewry, Pacific Exploratory Mission-West (PEM-West A): September-October 1991, *J. Geophys. Res.*, *101*, 1641-1653, 1996.

Hoell, J. M., D. D. Davis, S. C. Liu, R. E. Newell, H. Akimoto, R. J. McNeal, and R. J. Bendura, Pacific Exploratory Mission-West (PEM-West B): February-March 1994, *J. Geophys. Res.*, *102*, 28,223-28,239, 1997.

Hoell, J. M., D. D. Davis, D. J. Jacob, M. O. Rogers, R. E. Newell, H. E. Fuelberg, R. J. McNeal, J. L. Raper, and R. J. Bendura, Pacific Exploratory Mission in the tropical Pacific: PEM-Tropics A, August-September, 1996, *J. Geophys. Res.*, *104*, 5567-5583, 1999.

Hynes, A. J., E. A. Kenyon, A. J. Pounds, and P. H. Wine, Temperature-dependent absorption cross sections for acetone and normal butanone - Implications for atmospheric lifetimes, *Spectrochim. Acta*, *48*, 1235-1242, 1992.

Jacob, D. J., et al., Origin of ozone and NO_x in the tropical troposphere: A photochemical analysis of aircraft observations over the South Atlantic basin, *J. Geophys. Res.*, *101*, 24,235-24,250, 1996.

Jaeglé, L., et al., Observed OH and HO_2 in the upper troposphere suggest a major source from convective injection of peroxides, *Geophys. Res. Lett.*, *24*, 3181-3184, 1997.

Jaeglé, L., D. J. Jacob, W. H. Brune, D. Tan, I. C. Faloona, A. J. Weinheimer, B. A. Ridley, T. L. Campos, and G. W. Sachse, Sources of HO_x and production of ozone in the upper troposphere over the United States, *Geophys. Res. Lett.*, *25*, 1709-1712, 1998.

Johnston, H. S., C. A. Cantrell, and J. G. Calvert, Unimolecular decomposition of NO_3 to form NO and O_2 and a review of N_2O_5/NO_3 kinetics, *J. Geophys. Res.*, *91*, 5159-5172, 1986.

Kirstine, W., I. Galbally, Y. Ye, and M. Hooper, Emissions of volatile organic compounds (primarily oxygenated species) from pasture, *J. Geophys. Res.*, *103*, 10,605-10,619, 1998.

Lacis, A. A., D. J. Wuebbles, and J. A. Logan, Radiative forcing of climate by changes in the vertical distribution of ozone, *J. Geophys. Res.*, *95*, 9971-9981, 1990.

Liu, S. C., D. Kley, M. McFarland, J. D. Mahlman, and H. Levy II, On the origin of tropospheric ozone, *J. Geophys. Res.*, *85*, 7546-7552, 1980.

Logan, J. A., M. J. Prather, S. C. Wofsy, and M. B. McElroy, Tropospheric chemistry: A global perspective, *J. Geophys. Res.*, *86*, 7210-7254, 1981.

Lurmann, F. W., A. C. Lloyd, and R. Atkinson, A chemical mechanism for use in long-range transport/acid deposition computer modeling, *J. Geophys. Res.*, *91*, 10,905-10,936, 1986.

McKeen, S. A., T. Gierczak, J. B. Burkholder, P. O. Wennberg, T. F. Hanisco, E. R. Keim, R.-S. Gao, S. C. Liu, A. R. Ravishankara, and D. W. Fahey, The photochemistry of acetone in the upper troposphere: A source of odd-hydrogen radicals, *Geophys. Res. Lett.*, *24*, 3177-3180, 1997.

Molina, L. T., and M. J. Molina, Absorption cross sections of ozone in the 185 to 350 nm wavelength range, *J. Geophys. Res.*, *92*, 9740-9752, 1987.

O'Sullivan, D. W., M. Lee, B. C. Noone, and B. G. Heikes, Henry's law constant determinations for hydrogen peroxide, methylhydroperoxide, hydroxymethylhydroperoxide, ethylhydroperoxide, and peroxyacetic acid, *J. Phys. Chem.*, *100*, 3241-3247, 1996.

O'Sullivan, D. W., B. G. Heikes, M. Lee, W. Chang, G. Gregory, D. Blake, and G. Sachse, The distribution of hydrogen peroxide and methylhydroperoxide over the Pacific and South Atlantic Oceans, *J. Geophys. Res.*, *104*, 5635-5646, 1999.

Paulson, S. E., R. C. Flagan, and J. H. Seinfeld, Atmospheric photooxidation of isoprene Part I: The hydroxyl radical and ground state atomic oxygen reactions, *Int. J. Chem. Kinet.*, *24*, 79-101, 1992.

Pickering, K , J. R. Scala, A. M. Thompson, W.-K. Tao, and J. Simpson, A regional estimate of convective transport of CO from biomass burning, *Geophys. Res. Lett.*, *19*, 289-292, 1992.

Prather, M. J., and D. J. Jacob, A persistent imbalance in HO_x and NO_x photochemistry of the upper troposphere driven by deep tropical convection, *Geophys. Res. Lett.*, *24*, 3189-3192, 1997.

Roelofs, G.-J., J. Lelieveld, and R. van Dorland, A three-dimensional chemistry/general circulation model simulation of anthropogenically derived ozone in the troposphere and its radiative climate forcing, *J. Geophys. Res.*, *102*, 23,289-23,402, 1997.

Schultz, M. G., et al., On the origin of tropospheric ozone and NO_x over the tropical South Pacific, *J. Geophys. Res.*, *104*, 5829-5843, 1999.

Singh, H. B., D. O'Hara, D. Herlth, W. Sachse, D. R. Blake, J. D. Bradshaw, M. Kanakidou, and P. J. Crutzen, Acetone in the atmosphere: Distribution, sources, and sinks, *J. Geophys. Res.*, *99*, 1805-1819, 1994.

Singh, H. B., M. Kanakidou, P. J. Crutzen, and D. J. Jacob, High concentrations and photochemical fate of oxygenated hydrocarbons in the global troposphere, *Nature*, *378*, 50-54, 1995.

Siskind, D. E., M. E. Summers, and M. G. Mlynczak, An evaluation of $O_2(b^1\Sigma_g)$ as a possible source of OH and odd-nitrogen in the stratosphere and mesosphere, *Geophys. Res. Lett.*, *20*, 2047-2050, 1993.

Stevenson, D. S., W. J. Collins, C. E. Johnson, and R. G. Derwent, The impact of aircraft nitrogen oxide emissions on tropospheric ozone studied with a 3D lagrangian model including fully diurnal chemistry, *Atmos. Environ.*, *31*, 1837-1850, 1997.

Talukdar, R. K., C. A. Longfellow, M. K. Gilles, and A. R. Ravishankara, Quantum yields of $O(^1D)$ in the photolysis of ozone between 289 and 329 nm as a function of temperature, *Geophys. Res. Lett.*, *25*, 143-146, 1998.

Thompson, A. M., and R. W. Stewart, Effect of chemical kinetics uncertainties on calculated constituents in a tropospheric chemical model, *J. Geophys. Res.*, *96*, 13,089-13,103, 1991.

Thompson, A. M., H. B. Singh, R. W. Stewart, T. L. Kucsera, and Y. Kondo, A Monte Carlo study of upper tropospheric reactive nitrogen during the Pacific Exploratory Mission in the Western Pacific Ocean (PEM-West B), *J. Geophys. Res.*, *102*, 28,437-28,446, 1997.

Toumi, R., A potential new source of OH and odd-nitrogen in the atmosphere, *Geophys. Res. Lett.*, *20*, 25-28, 1993.

Vay, S. A., B. E. Anderson, G. W. Sachse, J. E. Collins, J. R. Podolske, C. H. Twohey, B. Gandrud, K. R. Chan, S. L. Baughcum, and H. A. Wallio, DC-8-based observations of aircraft CO, CH_4, N_2O, and H_2O(g) emission indices during SUCCESS, *Geophys. Res. Lett.*, *25*, 1717-1720, 1998.

Wang, W. C., D. J. Wuebbles, W. M. Washington, R. G. Isaacs, and G. Molnar, Trace gases and other potential perturbations to global climate, *Rev. Geophys.*, *24*, 110-140, 1986.

Wennberg, P. O., et al., Hydrogen radicals, nitrogen radicals, and the production of O_3 in the upper troposphere, *Science*, *279*, 49-53, 1998.

J. Barrick, J. Crawford, G. Gregory, J. Olson, and G. Sachse, NASA Langley Research Center, Hampton, VA, 23681 (email: j.h.crawford@larc.nasa.gov)

D. Blake, Department of Chemistry, University of California, Irvine, CA, 92717.

G. Chen, D. Davis, S. Liu, and S. Sandholm, School of Earth and Atmospheric Sciences, Georgia Institute of Technology, Atlanta, GA, 30332.

B. Heikes, Center for Atmospheric Chemistry Studies, University of Rhode Island, Narragansett, RI, 02882.

H. Singh, NASA Ames Research Center, Moffett Field, CA, 94035.

(Received November 20, 1998; revised February 17, 1999; accepted February 18, 1999.)